Ontogeny and innervation patterns of dopaminergic, noradrenergic, and serotonergic neurons in larval zebrafish

ARTICLE *in* THE JOURNAL OF COMPARATIVE NEUROLOGY · NOVEMBER 2004

Impact Factor: 3.23 · DOI: 10.1002/cne.20280 · Source: PubMed

THE JOURNAL OF COMPARATIVE NEUROLOGY 480:38–56 (2004)

Ontogeny and Innervation Patterns of Dopaminergic, Noradrenergic, and Serotonergic Neurons in Larval Zebrafish

DAVID L. McLEAN AND JOSEPH R. FETCHO*
Department of Neurobiology and Behavior, Life Sciences Building, State University of New York at Stony Brook, Stony Brook, New York 11794-5230

ABSTRACT

We report the development of aminergic neurons from 0–10 days postfertilization (dpf) in zebrafish (*Danio rerio*). This study was prompted by the lack of information regarding patterns of spinal aminergic innervation at early stages, when the fish are accessible to optical, genetic, and electrophysiological approaches toward understanding neural circuit function. Our findings suggest that aminergic populations with descending processes are among the first to appear during development. Descending aminergic fibers, revealed by antibodies to tyrosine hydroxylase (TH) and serotonin (5-hydroxytryptamine; 5-HT), innervate primarily the ventral (TH, 5-HT), but also the dorsal (5-HT) aspects of the spinal cord by 4 dpf, with the extent of innervation not changing markedly up to 10 dpf. By tracking the spatiotemporal expression of TH, 5-HT, and dopamine beta hydroxylase reactivity, we determined that these fibers likely originate from neurons in the posterior tuberculum (dopamine), the raphe region (5-HT) and, possibly, the locus coeruleus (noradrenaline). In addition, spinal neurons positive for 5-HT emerge between 1–2 dpf, with processes that appeared to descend along the ventrolateral cord for only 1–2 muscle segments. Their overall morphology distinguished these cells from previously described "VeMe" (ventromedial) interneurons, which are also located ventromedially, but have long, multisegmental descending processes. We confirmed the distinction between spinal serotonergic and VeMe interneurons using fish genetically labeled with green fluorescent protein. Our results suggest that the major aminergic systems described in adults are in place shortly after hatching, at a time when zebrafish are accessible to a battery of techniques to test neuronal function during behavior. J. Comp. Neurol. 480:38–56, 2004.

Indexing terms: neuromodulation; amines; brainstem; spinal cord; locomotion

While the spinal cord is the principle conduit for locomotor output, a great deal of the development, selection, and execution of different movements is orchestrated by descending inputs from the brain (Grillner, 1985; Pearson, 1993; Grillner and Wallén, 2002). The aminergic neuromodulators dopamine (DA), serotonin (5-hydroxytryptamine; 5-HT), and noradrenaline (NA) in particular have been implicated in the maturation and modulation of spinal networks (Sillar et al., 1998; Cazalets et al., 2000; Schmidt and Jordan, 2000; Vinay et al., 2000; Kudo et al., 2004). In rats, for example, the development of postural control and walking closely matches the spatiotemporal invasion of raphespinal inputs to the lumbar spinal column (Lakke, 1997). Early disruption of these inputs either chemically (Pflieger et al., 2002) or mechanically (Norreel et al., 2003) can cause serious disorganization of normal postural and stepping movements. Furthermore, combinations of different amines can activate and modulate rhythmic motor activity in the isolated mammalian spinal cord (Smith et al., 1988; Cazalets et al., 1990; Cowley and

Grant sponsor: National Research Service Award; Grant number: NS44728 (D.L.M.); Grant sponsor: National Institutes of Health; Grant number: NS26539 (J.R.F.).

Dr. David L. McLean's current address is Department of Neurobiology and Behavior, Mudd Hall, Cornell University, Ithaca, NY 14853.

Dr. Joseph R. Fetcho's current address is Department of Neurobiology and Behavior, Mudd Hall, Cornell University, Ithaca, NY 14853.

*Correspondence to: Joseph R. Fetcho, Department of Neurobiology and Behavior, Mudd Hall, Cornell University, Ithaca, NY 14853.
E-mail: jrf49@cornell.edu

Received 30 March 2004; Revised 15 June 2004; Accepted 23 June 2004

DOI 10.1002/cne.20280

Published online in Wiley InterScience (www.interscience.wiley.com).

Schmidt, 1994; Kiehn and Kjaerulff, 1996; Iizuka et al., 1998; Kiehn et al., 1999; Sqalli-Houssaini and Cazalets, 2000).

Investigations into the neuromodulation of spinal circuits using pharmacological and broad-scale lesion methods continue, but little is known about the natural activity patterns of aminergic populations and how they relate to motor control. If the ability to monitor the activity of identifiable neuromodulatory cells was combined with selective perturbations of their activity, compelling hypotheses about their function could not only be formulated, but also directly tested. This is presently difficult in mammals (Kiehn and Butt, 2003), but is possible in zebrafish because of the relative simplicity of their nervous system and their accessibility to optical, genetic, and electrophysiological approaches (Fetcho and O'Malley, 1995; O'Malley et al., 1996; Drapeau et al., 1999; Liu and Fetcho, 1999; Lorent et al., 2001; Ritter et al., 2001; Gahtan and O'Malley, 2003; Gleason et al., 2003; Higashijima et al., 2003).

Many of the published studies using zebrafish to date, however, have focused on the development and organization of their spinal (Bernhardt et al., 1990; Fetcho, 2001; Hale et al., 2001; Drapeau et al., 2002) and reticulospinal (Kimmel, 1982; Metcalfe et al., 1986; O'Malley et al., 1996; Ali et al., 2000; Gahtan et al., 2002) circuits, rather than on the roles of descending aminergic pathways. Aminergic populations have been described in zebrafish embryos and larvae (Guo et al., 1999, 2000; Holzschuh et al., 2001; Bellipanni et al., 2002; Rink and Wullimann, 2002), but little is known about the projection patterns of these populations, or their three-dimensional relationships, early in development. Here, we used tyrosine hydroxylase (TH), 5-HT, and dopamine beta hydroxylase (DβH) antibody labeling to identify potential spinal sources of DA, 5-HT, and NA, respectively. Our findings suggest that the full complement of aminergic systems described in adult fish (Van Raamsdonk et al., 1996; Kaslin and Panula, 2001; Rink and Wullimann, 2001) is present by 4–5 days postfertilization (dpf), at a time when the larvae have become free swimming, but are still accessible to the battery of technical approaches available in zebrafish. These data provide an anatomical framework to support functional studies of the aminergic modulation of neuronal circuits in larval fish.

MATERIALS AND METHODS

Zebrafish (*Danio rerio)* embryos and larvae were bred from a laboratory stock and maintained at 28.5°C on a 14-hour light / 10-hour dark cycle until 4 dpf, after which they were removed from the incubator and acclimated to room temperature (~22°C). After 5–6 dpf, larvae were raised on a diet of baby fish food (Tetra, Blacksburg, VA), as they have completely exhausted their yolk sac content by this time. Animals were staged according to Kimmel et al. (1995). Experiments were approved by the State University of New York-Stony Brook animal care committee and were in accord with National Institutes of Health guidelines.

Immunofluorescence processing

Embryos and larvae were first deeply anesthetized in 0.02% tricaine methanesulphonate (MS-222) in 10% Hank's solution and then fixed by immersion overnight in 4% formaldehyde in phosphate-buffered saline (PBS; pH 7.4) at 4°C. Fixed embryos up to 2 dpf were rinsed thoroughly in PBS and then quickly in distilled water before being dehydrated in a graded methanol series (10, 30, 50, 70, 90, and 100%), permeabilized in acetone for 5–10 minutes at –20°C, then rehydrated directly in PBS containing 0.5% Triton X-100 (TXPBS) and 5% normal goat serum (NGS). Fixed larvae from 2–10 dpf were pinned down through the notocord to a rotateable Sylgard-coated (Dow-Corning, Midland, MI) platform within a dissecting bath filled with PBS and the CNS was carefully excised using fine forceps and custom-etched tungsten dissecting pins. Due to the fragility of the spinal cord, the notocord and dorsal portion of the muscle myotomes were left intact to add support. All whole-mounts were subsequently blocked in 5% NGS/TXPBS overnight at 4°C.

To optimize double-immunofluorescent labeling, the tissue was processed in series, as recommended by Jackson ImmunoResearch (West Grove, PA). For example, after NGS block, whole-mounts were incubated in primary antiserum (in TXPBS) containing mouse anti-tyrosine hy-

Abbreviations

5-HT	5-hydroxytryptamine or serotonin
AC	anterior commissure
AP	area postrema
$apost_{CA}$	area postrema catecholaminergic group
Ce	cerebellum
d	diencephalon
DA	dopamine
DβH	dopamine beta hydroxylase
dpf	days postfertilization
DT	dorsal thalamus
E	epiphysis
EHT	endohypothalamic tract
H	hypothalamus
Hc(dm)	dorsomedial cell group of the caudal zone of the periventricular hypothalamus
Hi	intermediate hypothalamus
hpf	hours postfertilization
IR	inferior raphe
$infas_{CA}$	interfascicular catecholaminergic group
LC	locus coeruleus
OB	olfactory bulb
m	mesencephalon
NA	noradrenaline
P	pallium
PHT	preoptico-hypophyseal dopaminergic tract
Po	preoptic region
PoC	postoptic commissure
Pr	pretectal region
PT	posterior tuberculum
PTN	posterior tuberal nucleus
PVOa	periventricular organ-accompanying cells
r	rhombencephalon
Ra	raphe nuclei
SC	spinal cord
SP	subpallium
SR	superior raphe
t	telencephalon
TeO	optic tectum
TH	tyrosine hydroxylase
TPp	periventricular nucleus of the posterior tuberculum
$vagal_{CA}$	vagal catecholaminergic group
VT	ventral thalamus

droxylase (Chemicon International, Temecula, CA; 1:500–1:1000) for 2–4 days at 4°C, washed thoroughly all day in TXPBS, then incubated in secondary antiserum (in TXPBS) containing either goat anti-mouse conjugated to Cy-2 (Jackson ImmunoResearch; 1:200) or goat anti-mouse conjugated to Alexa Fluor-546 (Molecular Probes, Eugene, OR; 1:200) for 1–2 days at 4°C. The whole-mounts were washed in TXPBS, blocked again in 5% NGS/TXPBS, then incubated in primary antiserum containing either rabbit anti-serotonin (Sigma-RBI, St Louis, MO; 1:500) or rabbit anti-DβH (Chemicon International; 1:500) for 2–4 days at 4°C. They were then washed in TXPBS all day before incubation in secondary antiserum containing goat antirabbit conjugated to Cy-5 (Jackson ImmunoResearch; 1:200) for 1–2 days at 4°C. All whole-mounts were subsequently washed in several changes of TXPBS, rinsed in PBS, then oriented in 1.2% agar in 10% Hank's solution on the glass coverslip floor of a small Petri dish for confocal imaging (see below). The antibodies used here, although derived from mammalian sources, have been used successfully in adult zebrafish to label aminergic neural structures (Kaslin and Panula, 2001). As a negative control, several whole-mounts were processed with the primary antiserum steps omitted, which resulted in a complete absence of neuronal-specific staining, even at high confocal laser intensities (data not shown).

For cross-sectioning, the whole-mounts were removed from the agar, rinsed in PBS, and cryoprotected in a graded series of sucrose solution in PBS (5, 10, 20, and 30%). They were then oriented and frozen at –20°C in OCT cryomatrix (Miles, Elkhart, IN) and sections were cut on a freezing microtome (Cryocut 1800; Reichert-Jung, Nussloch, Germany) at 20–25 μm. Sections were then thaw-mounted on Superfrost-plus microscope slides (Fisher Scientific, Pittsburgh, PA), rinsed quickly in PBS to remove cryomatrix, coverslipped in 80% glycerol in PBS, and imaged immediately.

Transient expression of green fluorescent protein

Stochastic labeling of a limited number of spinal neurons with green fluorescent protein (GFP) was obtained using the neuronal-specific promoter *HuC* (Park et al., 2000). A DNA construct containing GFP driven by *HuC* (~25 ng/ml in distilled water; kindly provided by S. Higashijima) was injected into the cytoplasm of one-cell-stage zebrafish embryos as described previously in detail (Higashijima et al., 1997, 2003). Successful expression of GFP was determined at 2–3 dpf using an epifluorescence dissecting microscope. High-resolution preimages of GFP-labeled cells were obtained (see below for details) by first anesthetizing larvae in MS-222 and then embedding them laterally in 1.5% low-melting point agarose in 10% Hank's solution on a cover glass within a Petri dish. Larvae were subsequently processed for immunofluorescence as described above. GFP labeling persisted through anatomical processing.

Image acquisition and analysis

A Zeiss laser-scanning confocal imaging system (LSM 510; Zeiss, Thornwood, NY) was used to take optical sections of fluorescently labeled neurons. The agar mounting technique allowed us to orient the whole-mount according to the brain structures we wished to examine. Agar-embedded whole-mounts were covered in 10% Hank's solution to prevent the agar from desiccating. High-resolution images (1,024 × 1,024 pixels) were obtained in "multi track mode" (where images are captured sequentially, rather than simultaneously), to reduce the risks of nonspecific excitation of different fluorophores, using a combination of 488 nm excitation and a 505–550 nm bandpass filter (Cy-2, GFP), 543 nm excitation, and a 560 nm longpass filter (Alexa-546), 633 nm excitation, and a 650 nm longpass filter (Cy-5). A Plan-Neofluar 25× (0.8 numerical aperture, NA) water immersion lens was most commonly used, but for higher magnifications we used an Achroplan 40× (0.75 NA) water immersion lens.

For quantification of the total number of cells per aminergic population, we counted cells in a minimum of three fish at 5 and 10 dpf. Confocal imaging made it reasonably easy to distinguish and count single cells because we could reconstruct the cells from the optical sections through them. For measurements of the maximum cross-sectional area of the cell somata, we randomly selected five cells from each population per fish, in a minimum of three different fish, and an average was calculated using the Zeiss LSM 510 software (presented as mean ± standard error of the mean (SEM)). Stacks of optically sliced images were generated and pseudocolors were assigned using either Zeiss LSM 510 software or Adobe Photoshop (Adobe Systems, San Jose, CA). As an artifact of either collapsing the stacked optical slices using the confocal software, or individually importing optical slices into Photoshop and tiling them there, some montage images appear seamless, while others have noticeable edges. In both cases the total depth through the tissue within the image is reported in the appropriate legend. The resulting figures and schematics were prepared using CorelDraw (Corel, Dallas, TX).

RESULTS

Aminergic patterns of reactivity at 5 dpf

Since zebrafish larvae are sufficiently developed by 5 dpf to interact effectively with their environment (Kimmel et al., 1974, 1995; Budick and O'Malley, 2000), we used this as a starting point to describe the pattern of TH, 5-HT, and DβH immunoreactivity. Neurons and fibers positive for TH, but not DβH, are considered dopaminergic, while structures that are reactive for both are considered noradrenergic.

Telencephalon. Within the developing olfactory bulb (Figs. 1A, 2A), we observed a dense array of TH-reactive cells. TH reactivity here, and in other neuronal populations examined, was restricted to the cytoplasm. The labeled cells were slightly ovoid, just under 10 μm in diameter (maximum cross-sectional area, 52.2 ± 2.2 μm^2; n = 5), and had unipolar processes that appeared to ramify within glomeruli throughout the olfactory bulb (Figs. 1B1, 2B1). In close proximity to these olfactory bulb cells (Fig. 1E) were varicose 5-HT-reactive fibers concentrated largely in the dorsal region of the olfactory bulb (Figs. 1B2, 2B2). These varicosities originated from 5-HT fibers ascending within the lateral margins of the rostral diencephalon (Fig. 1B2,C2). This bilaterally located ascending bundle of 5-HT fibers was accompanied by TH-reactive fibers (Fig. 1C1-2,G), which also appeared to contribute to TH- and 5-HT-reactive neuropils throughout the subpallium (Figs. 1B1-2, 2B1-2). In the subpallium, a second

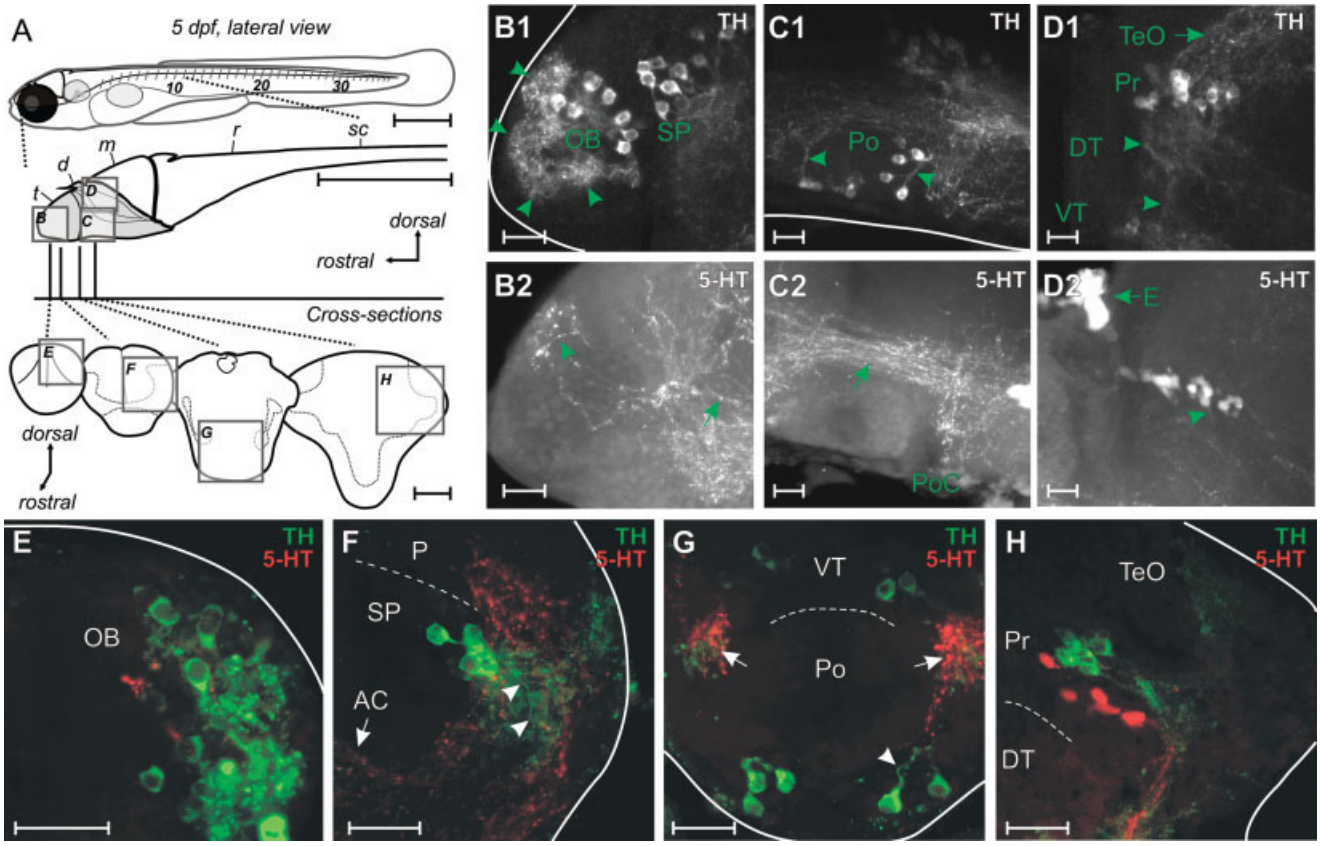

Fig. 1. Amine immunoreactivity in the telencephalon and rostral diencephalon at 5 dpf; cross-section and whole-mount lateral view. **A:** In the top panel, a schematic of a zebrafish larva illustrates the central nervous system and other major anatomical landmarks, including the eye (black circle), the otic capsule (oval with gray circles), the swim bladder (gray oval), and the intermyotomal clefts (numbered). In the middle panel, a schematic of the whole-mount nervous system divided into the telencephalon (t), diencephalon (d), mesencephalon (m), rhombencephalon (r), and spinal cord (sc), as first defined in Wullimann and Puelles (1999), illustrates the regions depicted in B–D. Arrows indicate orientation. In the bottom panel, traced outlines of cross-sections taken from the approximate regions indicated in the middle panel illustrate the regions depicted in E–H. Arrows indicate orientation. Here and in subsequent figures, dotted lines in the cross-section schematics illustrate the boundaries of white and gray matter. **B:** Photo montages derived from collapsed optical sections (50 μm) illustrate TH (B1) and 5-HT (B2) reactivity in the olfactory bulb (OB) and subpallium (SP). Green arrowheads in the olfactory bulb indicate the glomerular pattern of TH reactivity and the dorsal location of 5-HT reactivity, which appears to ascend from the rostral diencephalon (green arrow). Here and in subsequent figures, solid white lines demarcate the external boundaries of the nervous system. **C:** Collapsed optical sections (65 μm) illustrate TH (C1) and 5-HT (C2) reactivity in the preoptic region (Po), the lateral margin of the rostral diencephalon, and dorsolateral to and projecting within the postoptic commissure (PoC). Green arrowheads in C1 mark dorsal processes from the preoptic cells. **D:** Collapsed optical sections (75 μm) illustrate TH (D1) and 5-HT (D2) reactivity in the pretectum (Pr), optic tectum (TeO) and epiphysis (E) or pineal region. Green arrowheads indicate faint TH-reactive fibers running through the dorsal thalamus (DT) into the ventral thalamus (VT) and the faint ventral process from the pretectal 5-HT cells. **E:** Collapsed optical sections of a 20–25 μm cross-section through the olfactory bulb, as indicated in A (here and in subsequent figures, all images of cross-sections represent confocal stacks through the entire depth of tissue). Note the close proximity of 5-HT reactivity to TH-reactive cells. **F:** Cross-section through the pallium (P) and subpallium (SP), as indicated in A. White arrowheads indicate the ventrolateral processes of TH-reactive cells. Note the punctate TH and 5-HT reactivity projecting within the anterior commissure (AC). **G:** Cross-section through the preoptic region and the ventral thalamus, as indicated in A. A white arrowhead indicates the dorsal projections of the TH-reactive cells. Note the bundle of TH and 5-HT-reactive fibers coursing through the lateral margins of the rostral diencephalon (at white arrows). **H:** Cross-section through the pretectum, as indicated in A. Note the location of 5-HT-reactive cells immediately below TH-reactive ones in the pretectum, as well as TH reactivity in the optic tectum. In this and subsequent figures, white dashed lines demarcate the separation of brain regions, as defined in Wullimann and Peulles (1999). Scale bars = 0.5 mm in A (top); 50 μm in A (cross-sections); 20 μm in B1–H.

population of TH-reactive cells was obvious (Figs. 1B1, 2B1). These cells were similar in shape and size to the olfactory bulb neurons (maximum cross-sectional area, 51.9 ± 2.2 μm^2; n = 5); however, they were positioned more closely to the midline axis (Fig. 2B1). Their unipolar processes projected ventrolaterally (Fig. 1F), intermingling with the TH- and 5-HT-reactive fibers in the lateral margins of the telencephalon and within the anterior commissure (Figs. 1F, 2C1-2). We detected no DβH reactivity in the telencephalon.

Diencephalon. A number of TH-reactive cells were present in the preoptic region. The more rostral cells were oval-shaped, ~10 μm in diameter (maximum cross-sectional area, 50.2 ± 1.9 μm^2; n = 5), and were located ventrally, with unipolar processes that projected dorsally (Fig. 1C1), where they subsequently contributed to the

above-mentioned TH and 5-HT fibers within the lateral margins of the diencephalon and the anterior commissure. The more caudal cells in the preoptic region were the same shape, but had slightly larger cell bodies (maximum cross-sectional area, 54.9 ± 2.1 μm^2; n = 5), also with unipolar processes that projected dorsally (Fig. 1C1,G) where they joined TH and 5-HT fibers dorsal to the postoptic commissure (Fig. 1C1-2). This region at the lateral extremities and dorsal to the postoptic commissure was a prominent point of convergence for aminergic fibers, which made it difficult to discern their point of origin. From this region, tracts of fibers could be followed: 1) rostrally, forming the longitudinal bundles in the lateral margins of the rostral diencephalon that terminated in the telencephalon; 2) ventrally into the posterior tuberculum and hypothalamus; 3) dorsally, where they ran via the mesencephalon into the rhombencephalon (cf. Fig. 5B1-2); and 4) contralaterally, within the postoptic commissure (Figs. 1C1-2, 2C1-2).

In the pretectum, a discrete cluster of TH-reactive cells was observed. These neurons were tightly distributed along the midline axis (Fig. 2D1), similar to those of the subpallium, and were also similar in shape (Figs. 1D1, 2D1), but larger in size (maximum cross-sectional area, 60.2 ± 2.5 μm^2; n = 5). Their unipolar processes projected ventrolaterally and ramified in the dorsal thalamus, where they subsequently either projected commissurally just caudal to the epiphysis (Fig. 2D1) or projected to the optic tectum to form a dense plexus of TH fibers (Figs. 1D1, 2D1). A population of 5-HT-reactive cells was positioned just ventral to the TH cells in the pretectum (Fig. 1H). These were slightly smaller in size (maximum cross-sectional area, 51.7 ± 2.7 μm^2; n = 3), but similar in shape to the TH cells and also appeared to project ventrally (Fig. 1D2). Faint 5-HT-reactive fibers were also apparent crossing caudally to the epiphysis. In addition, there was punctate 5-HT reactivity in the optic tectum and strong 5-HT reactivity in the epiphysis (Figs. 1D2, 2D2). The 5-HT reactivity in these and all other 5-HT-reactive populations was observed throughout the cell, and not excluded from the nucleus, as was the TH reactivity.

The largest array of TH-reactive cells in the diencephalon ran contiguously from the ventral thalamus to the caudalmost region of the hypothalamus (Figs. 3A,B1, 4A,B1), with interposed, discrete 5-HT-reactive populations (Figs. 3B2, 4B2). There was clear heterogeneity within the TH array based on cell size, relative location, and projection profile. Beginning in the ventral thalamus and continuing into the ventral part of the posterior tuberculum (Fig. 3B1), one group formed a loose column relatively close to the midline (Figs. 3C, 4B1), which consisted of ovoid cells, 10–15 μm in diameter (maximum cross-sectional area, 60.3 ± 2.4 μm^2; n = 5) that had unipolar axons which projected ventrolaterally (Fig. 3C) to the plexus of TH fibers that ramified dorsal to the postoptic commissure (Fig. 3B1).

A second group of cells was located entirely within the posterior tuberculum (Fig. 3B1) and close to the midline

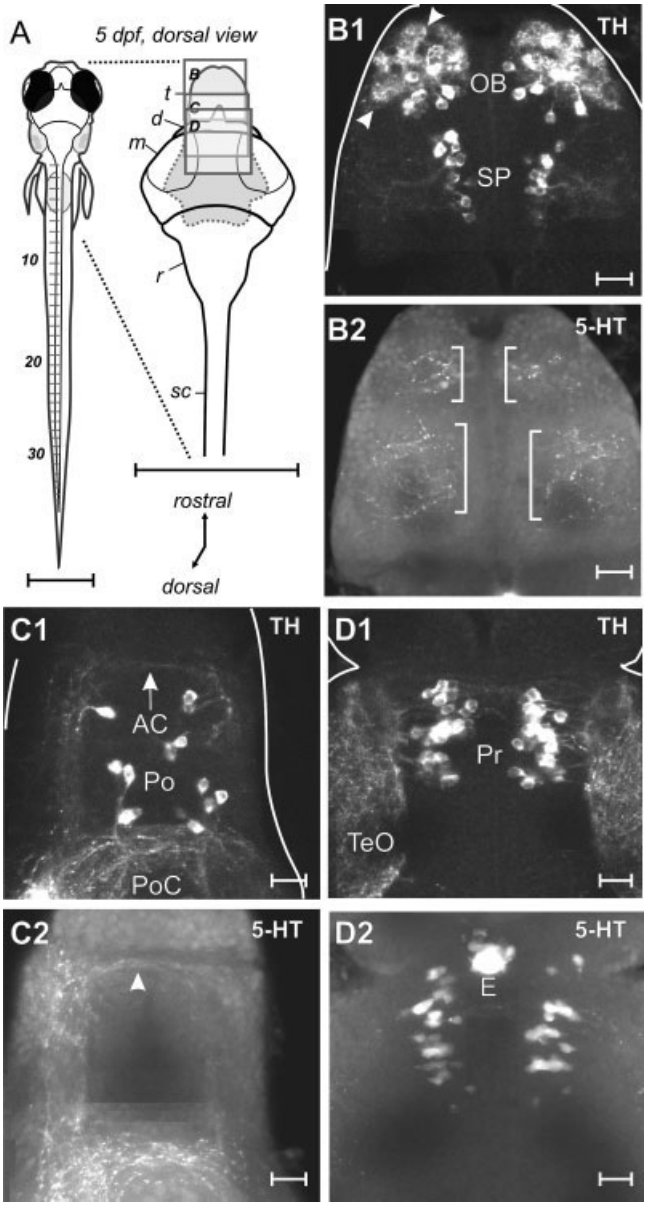

Fig. 2. Amine immunoreactivity in the telencephalon and rostral diencephalon at 5 dpf; whole-mount dorsal view. **A:** In the left panel, a schematic of a zebrafish larva illustrates the central nervous system and other major anatomical landmarks, including the eyes (black circles), the otic capsules (oval with gray circles), the swim bladder (gray oval), the pectoral fins, and the intermyotomal clefts (numbered). In the right panel, a schematic of the whole-mount nervous system divided into the telencephalon (t), diencephalon (d), mesencephalon (m), rhombencephalon (r), and spinal cord (sc), illustrates the regions depicted in B–D. Arrows indicate orientation. **B:** Photo montages derived from collapsed optical sections (50 μm) illustrate TH (B1) and 5-HT (B2) reactivity in the olfactory bulb (OB) and subpallium (SP). White arrowheads indicate the glomerular pattern of TH reactivity in the olfactory bulb. White brackets mark the presence of 5-HT reactivity in the olfactory bulb and subpallium. **C:** Collapsed optical sections (100 μm) illustrate TH (C1) and 5-HT (C2) reactivity in the preoptic region (Po). Note the faint TH and 5-HT reactivity within the anterior commissure (AC, at white arrowhead in C2), the postoptic commissure (PoC) and running longitudinally in the lateral diencephalon. Note also the intense labeling laterally at the level of the postoptic commissure. **D:** Collapsed optical sections (80 μm) illustrate TH (D1) and 5-HT (D2) in the pretectum (Pr). Note the TH reactivity in the optic tectum (TeO) and the intense 5-HT labeling in the epiphysis (E) or pineal region. Scale bars = 0.5 mm in A; 20 μm in B1–D2.

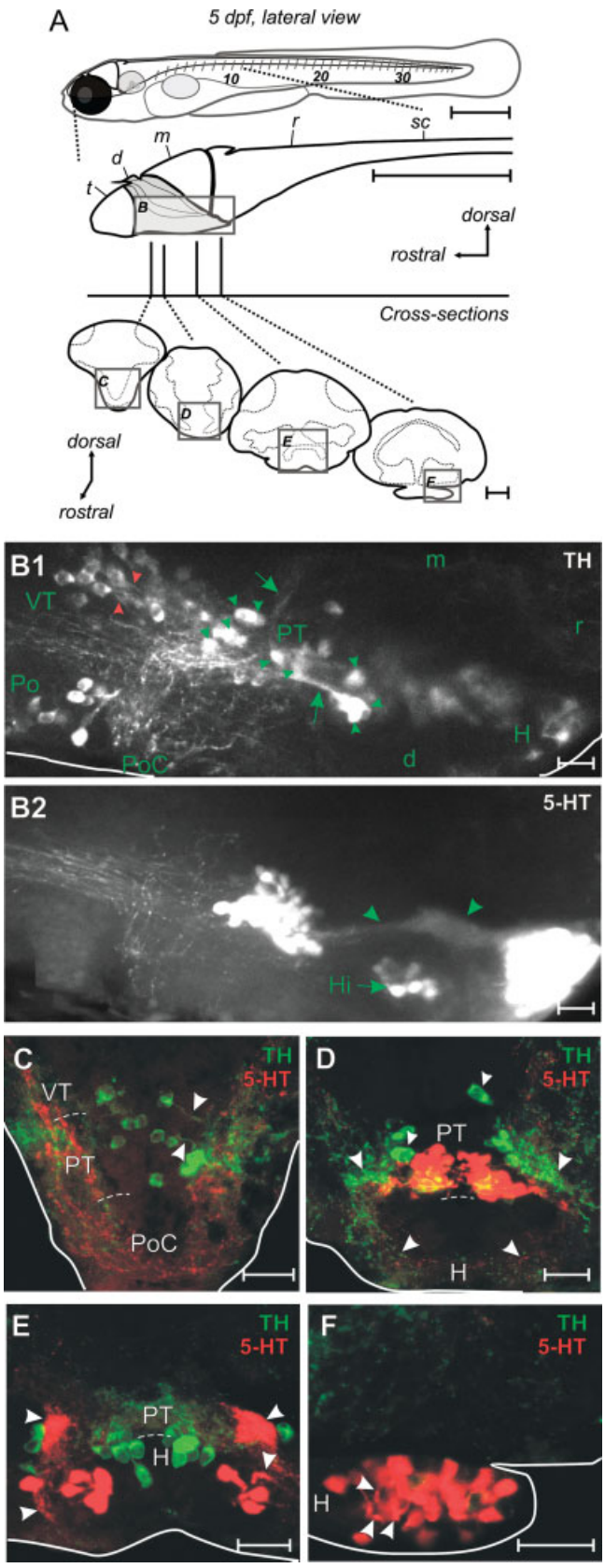

(Figs. 3D, 4B1), but the somata were much larger (maximum cross-sectional area, 107.1 ± 3.6 μm^2; n = 5). These large cells were also distinguishable by prominent processes that either projected dorsally (Figs. 3B1, 5D) into the bundle of TH and 5-HT fibers that continued via the mesencephalon into the rhombencephalon (Fig. 5B1-2), or rostrally (Fig. 3B1), contributing to the dense plexus of TH and 5-HT fibers dorsal to the postoptic commissure. In dorsoventral view, this population resembled parentheses (Fig. 4B1).

Overlapping this population, but running further into the hypothalamus (Fig. 3B1), was an array of slightly smaller, ovoid cells (maximum cross-sectional area, 59.1 ± 1.2 μm^2; n = 5) that were organized as a coherent, longitudinal column, near the midline (Figs. 3E, 4B1). These neurons gave rise to unipolar processes directed rostrodorsally (Fig. 4E), where they joined TH- and 5-HT-reactive fibers that coursed through the lateral margins of the ventral diencephalon. TH-reactive fibers were also observed on the pial or ventral surface of the hypothalamus (Figs. 3D,E, 4D), in addition to a prominent tract that connected the diencephalon directly to the rhombencephalon (Fig. 5B1).

At the caudalmost part of the hypothalamus (Fig. 4B1) was a population of small TH-reactive cells (maximum cross-sectional area, 37.9 ± 1.2 μm^2; n = 5), which had short, club-like dendritic processes (Figs. 3F, 4F). Cells of

Fig. 3. Amine immunoreactivity in the ventral diencephalon at 5 dpf; cross-section and whole-mount lateral view. **A:** Schematic drawings of a zebrafish larva (top panel), the whole-mount nervous system (middle panel) and the resulting cross-sections (bottom panel) that illustrate the regions depicted in B–F. For more details, see Figure 1 legend. Arrows indicate orientation. **B:** Photo montages derived from collapsed optical sections (80 μm) illustrate TH (B1) and 5-HT (B2) in the ventral diencephalon. Green arrows indicate dorsal and rostral projections from large TH-reactive posterior tuberculum (PT) cells (at small green arrowheads). Large green arrowheads indicate the 5-HT-reactive tract that courses through the hypothalamus (H) and posterior tuberculum. Note the smaller TH-reactive cells in the ventral thalamus (VT) that send their processes ventrocaudally (small red arrowheads), where they join TH-reactive fibers from the preoptic region (Po) that intermingle dorsal to the postoptic commissure (PoC). TH-reactive cells are also present in the intermediate hypothalamus (Hi) and hypothalamus, along with 5-HT-reactive cells. **C:** Cross-section through the ventral thalamus, posterior tuberculum, and postoptic commissure, as indicated in A. Note the ventrolateral projections of the TH-reactive cells in the ventral thalamus (white arrowheads) and the TH and 5-HT reactivity within the postoptic commissure and the lateral margins of the diencephalon. **D:** Cross-section through the posterior tuberculum and hypothalamus. Large white arrowheads indicate the TH- and 5-HT-reactive fibers coursing through the lateral aspects of the diencephalon and along its ventral or pial surface. Small white arrowheads indicate the large TH-reactive cells in the posterior tuberculum. Note that due to the high laser intensity needed to observe the faintly labeled processes, overlapping 5-HT reactivity (in red) and TH reactivity (in green) in this 25-μm cross-section gives a false impression of colocalization, as suggested by the yellow color. The cell bodies are in close proximity, but different optical planes (cf. Fig. 4). **E:** Cross-section through the posterior tuberculum and hypothalamus. White arrowheads note laterally located TH and 5-HT-reactive processes and fibers. Note how close the TH-reactive cells are to the midline. Note also the dense concentration of 5-HT-reactive processes (top arrows; see also green arrows in B2). **F:** Cross-section through the hypothalamus. White arrowheads indicate the club-like dendritic processes of the 5-HT-reactive cells. Scale bars = 0.5 mm in A (top panel); 50 μm in A (cross-sections); 20 μm in B1–F.

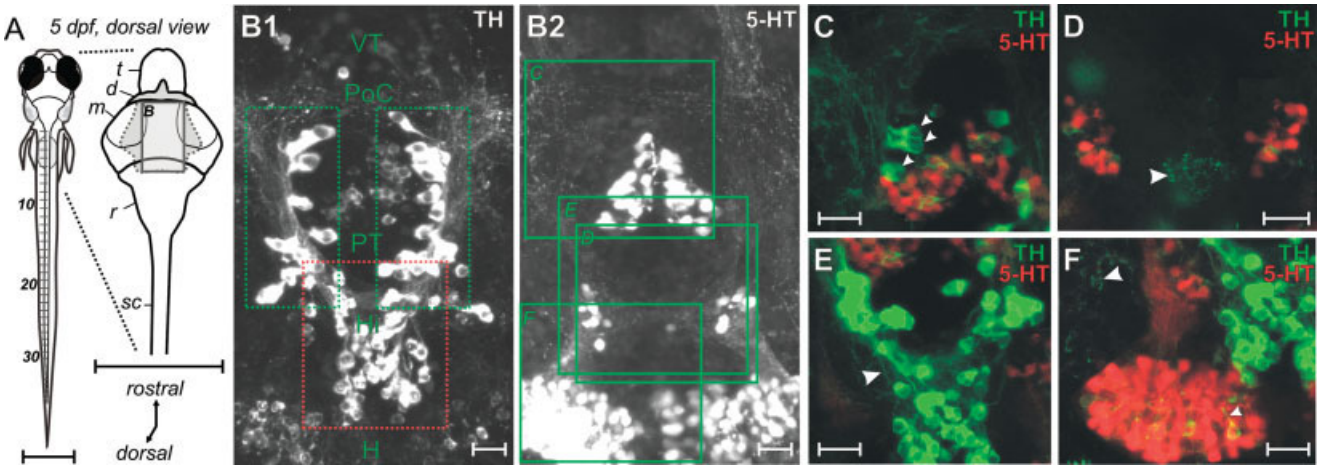

Fig. 4. Amine immunoreactivity in the ventral diencephalon at 5 dpf; whole-mount dorsal view. **A:** Schematic drawings of a zebrafish larva (left panel) and the whole-mount nervous system (right panel) that illustrate the region depicted in B. For more details, see Figure 2 legend. Arrows indicate orientation. **B:** Photo montages derived from collapsed optical sections (80 μm) illustrate TH (B1) and 5-HT (B2) in the ventral diencephalon. While B1 and B2 are taken from the same fish, green boxes in B2 are present to indicate the approximate regions depicted in C-F, which are taken from a different preparation. These images were selected because they were taken using a higher-magnification lens. Note the TH-reactive neurons in the ventral thalamus (VT) that appear more dimly labeled due to their depth within the tissue and the TH and 5-HT reactivity ramifying laterally at the level of the postoptic commissure (PoC), which is comprised of fibers from the large posterior tuberculum (PT) cells (in green dotted boxes). These large cells form parentheses, within which can be found TH and 5-HT-reactive cells. Further caudally is another population of TH-reactive cells that overlap with the large posterior tuberculum cells (in red dotted box) in the intermediate hypothalamus (Hi), located close to the midline. More laterally in this region are 5-HT-reactive cells. Populations of TH- and 5-HT-reactive cells are also located in the caudalmost aspect of the hypothalamus (H). **C:** Collapsed optical sections (50 μm) illustrate TH and 5-HT reactivity in the rostral region of the ventral posterior tuberculum. Small white arrowheads indicate the large posterior tuberculum cells. **D:** Collapsed optical sections (25 μm) illustrate TH and 5-HT reactivity in the rostral hypothalamus. White arrowhead indicates TH reactivity on the ventral or pial surface of the hypothalamus, possibly exiting into the pituitary. **E:** Collapsed optical sections (50 μm) illustrate TH and 5-HT in the caudal region of the ventral posterior tuberculum. A white arrowhead indicates a prominent rostral projection from the intermediate hypothalamus TH-reactive population. **F:** Collapsed optical sections (40 μm) illustrate TH and 5-HT reactivity in the caudal hypothalamus. A white arrowhead indicates TH-reactive fibers in the lateral hypothalamus and a small white arrowhead marks the club-like dendrite of a TH-reactive neuron in the caudal hypothalamus. Scale bars = 0.5 mm in A; 20 μm in B1–F.

a similar morphology and size (maximum cross-sectional area, 36.8 ± 2.3 μm^2; n = 5) could also be found in the posterior tuberculum (Fig. 4B1,C). These diencephalic cell types resemble those previously described in cross-section as "small round," large "pear-shaped," and "bipolar liquor contacting" neurons (Rink and Wullimann, 2001, 2002).

Within the ventral part of the posterior tuberculum (Fig. 3B2), a cluster of 5-HT cells, resembling an arrowhead from the dorsoventral perspective (Fig. 4B2), was enclosed by the parenthetic group of large TH cells (Fig. 4B1-2,C). These cells were around 5–10 μm in diameter (maximum cross-sectional area, 41.6 ± 1.5 μm^2; n = 3), and had club-like dendritic processes that concentrated at the middle of the population (Fig. 3D) and axons that projected laterally joining the TH and 5-HT fibers in the lateral margins of the caudal diencephalon (Fig. 4B1-2).

In the hypothalamus two distinct populations of 5-HT cells were observed. The first was located in the intermediate hypothalamus (Figs. 3B2, 4D) and consisted of small cells (maximum cross-sectional area, 34.7 ± 1.4 μm^2; n = 3) with club-like dendrites and laterally projecting axons. The second population was located in the caudalmost aspect of the hypothalamus (Fig. 3B2) and had a cell size (maximum cross-sectional area, 36.4 ± 1.1 μm^2; n = 3) and a morphology that bore a striking resemblance to the aforementioned bipolar liquor contacting TH cells (Figs. 3F, 4F). While TH- and 5-HT-reactive fibers and cell bodies were in very close proximity, it was clear that they did not colocalize in the diencephalon (Fig. 4C-F). There were, however, a great many more 5-HT cells present in the caudal hypothalamus than TH-reactive cells. Remarkably, as in the telencephalon, we could detect no DβH reactivity in the diencephalon.

Mesencephalon. The only pattern of TH and 5-HT reactivity observed in the mesencephalon at this stage of development was tracts of aminergic fibers, presumably derived from populations in the diencephalon and rhombencephalon (Fig. 5A,B1-2). In the optic tectum, TH-reactive fibers were concentrated mainly in the dorsal- and ventralmost regions (Fig. 5C). Meanwhile, punctate 5-HT reactivity could be detected throughout the tectum (Fig. 5C). TH and 5-HT fibers were found in the lateral regions of the mesencephalon (Fig. 5E); the prominent tracts of aminergic fibers that connected the diencephalon to the rhombencephalon ran more ventrally (Fig. 5B1-2) and medially (Fig. 5D). TH- and 5-HT-reactive fibers coursing through the mesencephalon were loosely organized as bundles, with TH-reactive fibers generally concentrated more medially than the 5-HT-reactive ones (Fig. 5D-E). Again, we could detect no DβH reactivity in the mesencephalon.

Rhombencephalon. Moving caudally, the first TH-reactive population observed near the mesencephalon/rhombencephalon border was the anatomically distinctive locus coeruleus (Figs. 6A,B1, 7A,B2). At 5 dpf the cell bodies were teardrop-shaped (Fig. 6F), ~15 μm in diam-

eter (maximum cross-sectional area, 94.2 ± 5.0 μm^2; n = 5), located ventromedially (Figs. 6B1, 7B2), with single unipolar processes that projected ventrally (Fig. 6F), and contributed to the series of TH-reactive fiber tracts (Figs. 6F, 7B2). The close proximity of 5-HT reactivity to, presumably, the dendritic processes of the locus coeruleus indicated likely aminergic interaction (Fig. 6F). We confirmed that these cells were noradrenergic by their coexpression of DβH reactivity (Fig. 6B3,C1). On no occasion did we observe TH reactivity in the absence of DβH reactivity in this region (Figs. 6L1-3, 7G1-3). DβH reactivity, however, was confined to the cell body and the initial axon segment (Fig. 6C1,L1-3), so DβH-reactive processes were not robust. By contrast, there was an extensive amount of TH reactivity coursing throughout the rhombencephalon. Tracts could be observed ascending at the level of the locus coeruleus (Fig. 7D), where they innervated the cerebellum (Fig. 6D), and ramified more caudally at the level of the otic capsule (Fig. 6B1,G). In addition to these dorsal locations, TH reactivity was also concentrated in the rostral medulla (Fig. 7B2), in close proximity to serotonergic raphe neurons (Figs. 6E, 7E), making aminergic interactions likely. TH reactivity was also observed coursing longitudinally (Fig. 7B2), along the ventrolateral medulla (Fig. 6H-I). Also apparent were decussating fibers, with what appeared to be a segmental organization (Fig. 7B2).

In the caudal rhombencephalon, a second population of TH-reactive cells could be detected. These cells began at the level of the otic capsule and extended through the area postrema to the spinomedullary border (Figs. 6B1, 7C2), forming the shape of an inverted horseshoe when observed from the dorsoventral perspective (Fig. 7C2). All of these cells in the caudal medulla were consistently the same size (maximum cross-sectional area, 59.6 ± 3.9 μm^2; n = 5) and generally resembled those in the locus coeruleus in that they were teardrop-shaped, with long ventrally projecting processes that joined the longitudinal tracts of TH-reactive fibers (Fig. 6B1). TH-reactive fibers were also detected originating from this region that ramified dorsally, in the area postrema (Fig. 6B1), and projected commissurally at the spinomedullary border (Fig. 7C2). Notably, two distinctions could be made within this large group of cells. The first was a small subpopulation offset from the rest, nearer the midline (Fig. 7C2,F). The second was cells tightly clustered at the spinomedullary border, whose close proximity to one another made it difficult to definitively discern single processes (Fig. 6J). We also confirmed that a proportion of this population were noradrenergic by DβH co-reactivity (Fig. 6C2). Like the locus

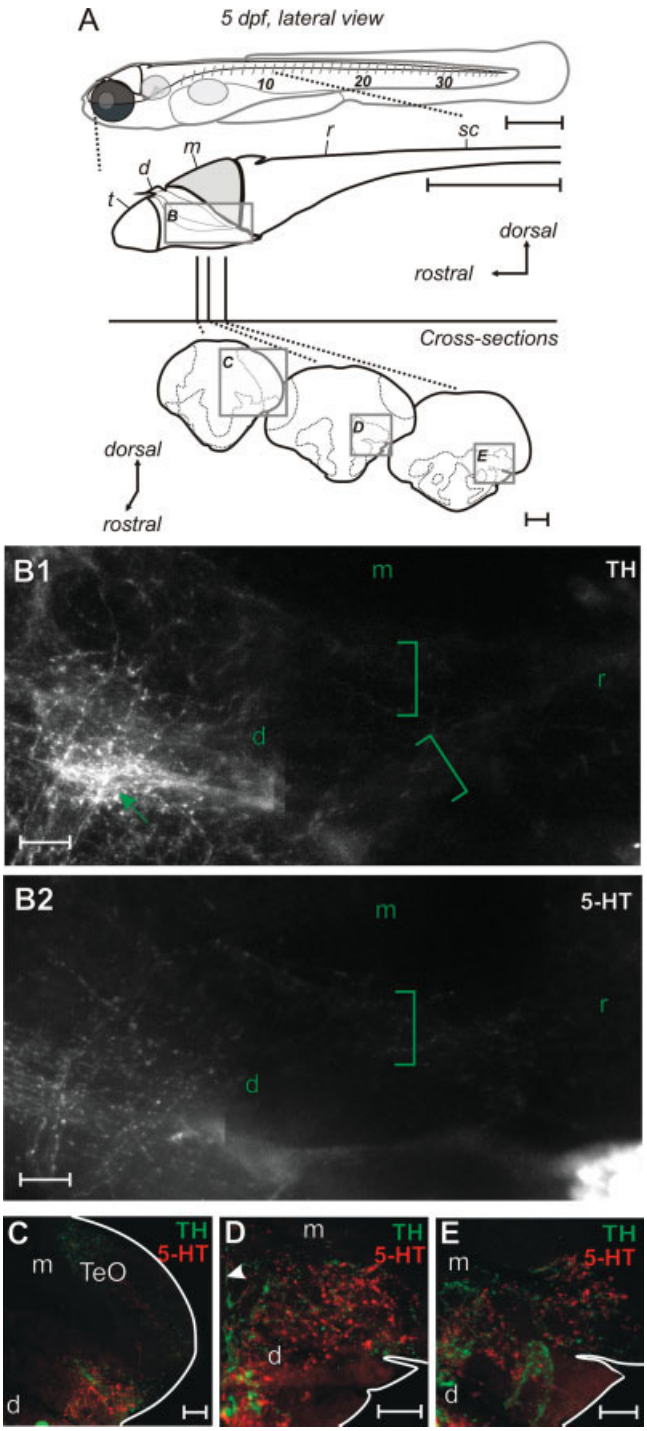

Fig. 5. Amine immunoreactivity in the mesencephalon at 5 dpf; cross-section and whole-mount lateral view. **A:** Schematic drawings of a zebrafish larva (top panel), the whole-mount nervous system (middle panel) and the resulting cross-sections (bottom panel), illustrate the regions depicted in B–E. For more details, see Figure 1 legend. Arrows indicate orientation. **B:** Photo montages derived from collapsed optical sections (72 μm) illustrate TH (B1) and 5-HT (B2) reactivity in the ventral mesencephalon. Green brackets indicate the faint aminergic fibers that pass through the mesencephalon (m) and diencephalon (d) into the rhombencephalon (r). Note that for TH reactivity, more ventrally fibers are also apparent that directly connect the diencephalon to the rhombencephalon (lower green bracket). A green arrow indicates the aminergic fibers that ramify dorsal to the postoptic commissure. **C:** Cross-section through the optic tectum (TeO), as indicated in A. Note the TH- and 5-HT-reactive fibers in the optic tectum, as well as fibers that course longitudinally through the lateral diencephalon. **D:** Cross-section through the mesencephalon illustrating the tracts of TH and 5-HT-reactive axons. A white arrowhead indicates a prominent TH fiber ascending from the posterior tuberculum (PT). **E:** Cross-section through the mesencephalon. Many aminergic fibers can be noted coursing longitudinally through the ventral mesencephalon and immediately below, in the diencephalon. Scale bars = 0.5 mm in A (top); 50 μm in A (cross-sections); 20 μm in B1–E.

coeruleus, DβH reactivity was only noted in the cell body and initial axon segment (Fig. 6C2), but unlike the locus coeruleus there were often TH-reactive neurons that did not display DβH reactivity (Figs. 6M1-3, 7H1-3). This makes it likely that this region contains both dopaminergic and noradrenergic neurons. Finally, TH-reactive fibers were observed entering the spinal cord (Fig. 6K).

The highest concentration of 5-HT reactivity was in the rhombencephalon. Immediately below the cerebellum was a small population of cells (Fig. 6B2). These cells were tightly packed together, making it difficult to discern single cells (Fig. 6D), and appeared to be connected by a prominent commissure (Fig. 7D). Immediately below this region began the largest population of 5-HT-reactive cells, the serotonergic raphe region, which extended almost contiguously to the spinal cord. From a dorsoventral perspective, these cells appeared to be organized as a longitudinal column, broken into clusters (Fig. 7B1). From a lateral perspective (Fig. 6B2) and in cross-section (Fig. 6E,H,I), however, it was apparent that cells were loosely distributed along the dorsoventral plane. Within this population was clear heterogeneity, based on location and cell size. The larger 5-HT-reactive cells (maximum cross-sectional area, 53.9 ± 0.6 μm^2; n = 3) were more rostral (red asterisk in Fig. 7B1) and dorsal (red asterisk in Fig. 6B2), and located close to the midline (Fig. 7B1). Fine varicose processes extended from these cells ventrolaterally (Fig. 6E), which joined 5-HT-reactive fibers with very similar projection patterns to the above-mentioned TH-reactive fibers. For instance, 5-HT reactivity was detected ascending to the cerebellum (Figs. 6D, 7D), ramifying dorsally at the level of the otic capsule (Fig. 6B2,G) and running ventrolaterally (Fig. 6H,I), where a segmental distribution was also apparent (Fig. 7B1). Overlapping the large subpopulation of 5-HT neurons was a second group of topographically distinct 5-HT cells (green asterisks in Figs. 6B2, 7B1). These cells were smaller in size (maximum cross-sectional area, 36.6 ± 1.2 μm^2; n = 3) and could also be found close to the ventral surface of the rhombencephalon, unlike the aforementioned larger, 5-HT-reactive cells (Fig. 6B2). These cells too were located close to the midline (Figs. 6H,I, 7B1) and were organized in a segmental manner, with gaps between subsequent segments (Figs. 6B2, 7B1), which corresponded closely to 5-HT-reactive fibers that ramified within the same segment (Fig. 7B1). Another distinct population of 5-HT-reactive cells was located caudally, in the dorsal hindbrain (red dotted box in Fig. 6B2, bracketed in Fig. 6G,I), close to the TH- and DβH-reactive populations in the area postrema. Like those populations, the 5-HT-reactive population could also be subdivided into cells located closer to the midline versus cells located closer to the periphery (Fig. 7C1,F). These 5-HT cells too were small (maximum cross-sectional area, 33.0 ± 1.0 μm^2; n = 3) and had fine varicose processes that joined 5-HT fibers in the dorsolateral margins of the rhombencephalon, and also appeared to decussate at the spinomedullary boundary (Fig. 7C1). However, in contrast to the TH- and DβH-reactive cells, the 5-HT-reactive neurons were more rostral and dorsal (Fig. 6B1-2) and did not extend to the spinomedullary border (Figs. 6B2, 7C1).

Spinal cord. There were no TH-reactive cells detectable in spinal cord, but there were many TH fibers coursing predominantly through its ventrolateral aspects (Fig. 8A,B1-3), which continued to the caudalmost extremity of the cord (Fig. 8C1,D1,E1). However, in the rostral spinal cord we observed occasional TH-reactive fibers more dorsally (Fig. 8B1). As in the brain, we could not detect any robustly labeled DβH fibers in the spinal cord. In contrast, there were two tracts of 5-HT-reactive fibers. The first ran along the dorsal aspect of the lateral margin almost the whole length of the spinal cord (to ~25th muscle segment; Fig. 8B1-2,D2) and appeared contiguous with fibers originating from the brain (Fig. 8C2). The second overlapped with the TH-reactive fibers in the ventral aspect of the lateral margin (Fig. 8B1,C1-2), and similarly ran the whole length of the spinal cord (to ~35th muscle segment; Fig. 8E2). The ventral fibers could have originated from two sources: 5-HT-reactive cells in the brain and 5-HT-reactive cells located within the spinal cord. The varicose, punctate nature of 5-HT reactivity made it difficult to follow individual tracts, so we cannot completely rule out

Fig. 6. Amine immunoreactivity in the rhombencephalon at 5 dpf; cross-section and whole-mount lateral views. **A:** Schematic drawings of a zebrafish larva (top panel), the whole-mount nervous system (middle panel), and the resulting cross-sections (bottom panel) that illustrate the regions depicted in B and D–K. For more details, see Figure 1 legend. Arrows indicate orientation. **B:** Photo montages derived from collapsed optical sections (80 μm, left portion of composite; 120 μm, right portion of composite) illustrate TH (B1) and 5-HT (B2) reactivity in the rhombencephalon. For DβH (B3), collapsed optical sections (75 μm, left portion of composite; 75 μm, right portion of composite) are presented from a different preparation. Green arrowheads in B1-2 indicate dorsal aminergic fibers just above the plane of focus for the left portion of the composite images. Red and green asterisks in B2 are placed above the rhombomeric clustering of raphe neurons (Ra). A green asterisk in B1 also notes the locus coeruleus (LC). Red-dotted boxes illustrate the TH- and 5-HT-reactive populations located near the area postrema (AP) in the caudal rhombencephalon. **C:** Higher magnification of regions indicated by green boxes in B3 illustrate the restriction of DβH to the somata and initial segment. **D:** Cross-section through the region of the cerebellum (Ce), as indicated in A. White arrowheads indicate the ascending TH-reactive fibers and the intensely labeled 5-HT-reactive cell bodies, which are densely packed together, making them difficult to individually identify in cross-section. **E:** Cross-section through the rostral raphe region (Ra). Note the close proximity of TH-reactive fibers to the raphe cell bodies. A white arrowhead indicates ventrolateral process. **F:** Cross-section illustrating the locus coeruleus. **G:** Cross-section illustrating the dorsolateral rhombencephalon. A white bracket indicates the dorsal 5-HT cells and a white arrowhead notes the dorsal TH and 5-HT-reactive fibers. **H:** Cross-section illustrating the ventromedial rhombencephalon. Note the dorsoventral positioning of the small, caudal raphe cells and the tracts of 5-HT and TH fibers running through the lateral aspects of the rhombencephalon. **I:** More caudal cross-section through the rhombencephalon. A white bracket indicates dorsal 5-HT cells. **J:** Cross-section through the area postrema (AP) in the caudal rhombencephalon. TH-reactive cells near the spinomedullary border are packed tightly together, making it difficult to discern their processes. **K:** Cross-section through the very caudal rhombencephalon. Note the ventrally positioned TH and 5-HT-reactive fibers that will enter the spinal cord. **L:** A cross-section from a different preparation illustrates that TH (L1) and DβH (L2) colocalize in the locus coeruleus (L3). Note that the DβH staining is restricted to the soma and initial segment. Note also that there is a higher level of background fluorescence in the DβH-stained tissue. **M:** A cross section from a different preparation illustrates that TH (M1) and DβH (M2) often, but not always, colocalize in the area postrema (M3). Scale bars = 0.5 mm in A (top); 50 μm in A (cross-sections), B; 20 μm in C–M.

the contribution of descending inputs to ventral 5-HT innervation (or that some of the dorsal innervation also comes from the spinal 5-HT cells).

At this stage, the spinal 5-HT-reactive cells began just inside the spinomedullary border, at the level of the 1st–2nd muscle segment, and were evenly distributed along the whole length of the spinal cord, as determined by cell counts between the 3rd–8th (2.2 ± 0.1 per segment; n = 5), 13th–18th (2.5 ± 0.2 per segment; n = 5) and 23rd–28th (2.2 ± 0.1 per segment; n = 5) muscle segments. They were also consistently the same size in these regions (~10 μm in diameter maximum cross-sectional area, 3rd–8th, 53.8 ± 1.2 μm^2; 13th–18th, 49.3 ± 2.1 μm^2; 23rd–28th, 51.8 ± 1.8 μm^2; n = 5), oval (or circular, depending on the viewing angle) shaped, and located ventrally and medially, close to the central canal (Fig. 8B3). They had a

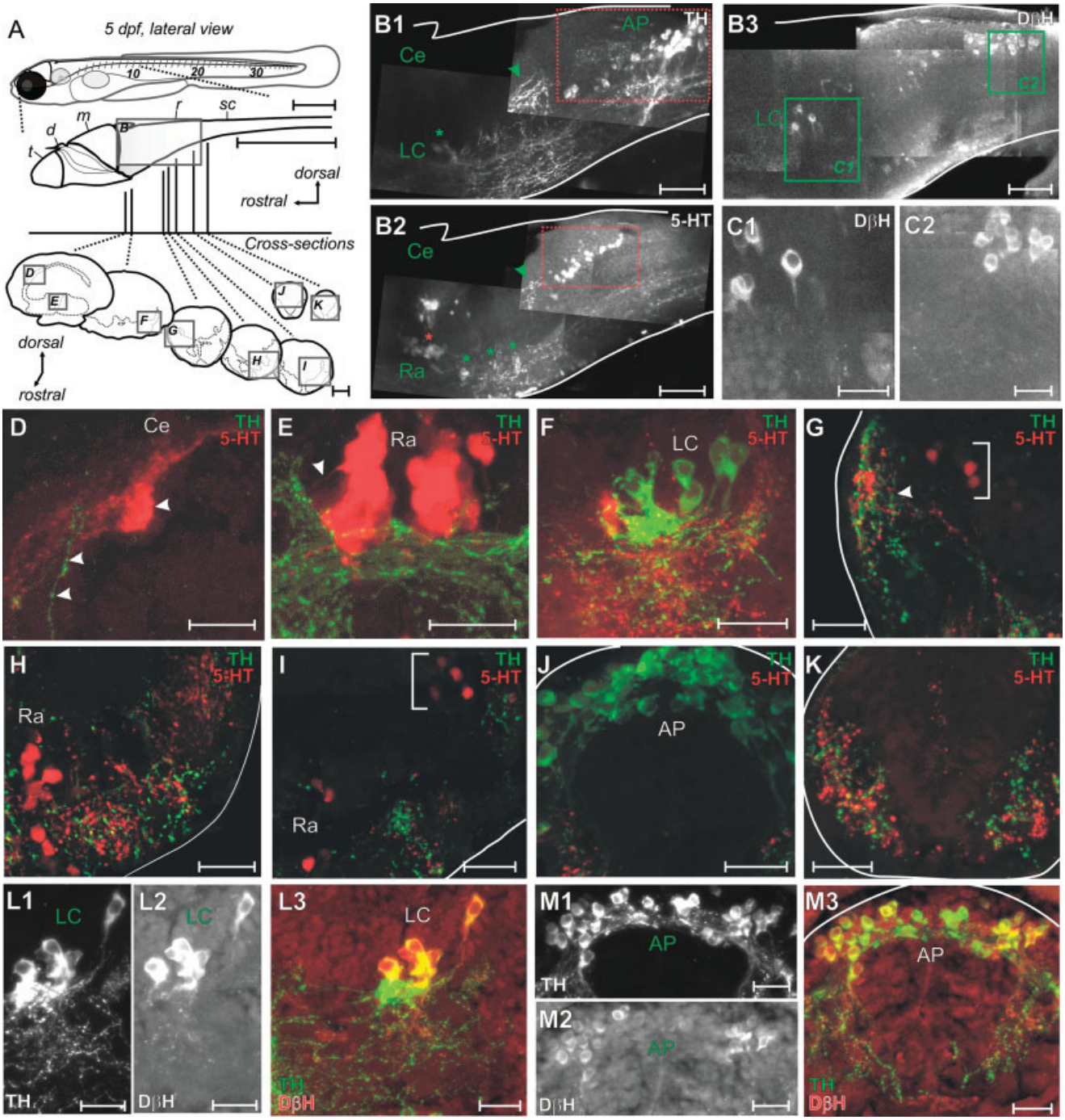

Figure 6

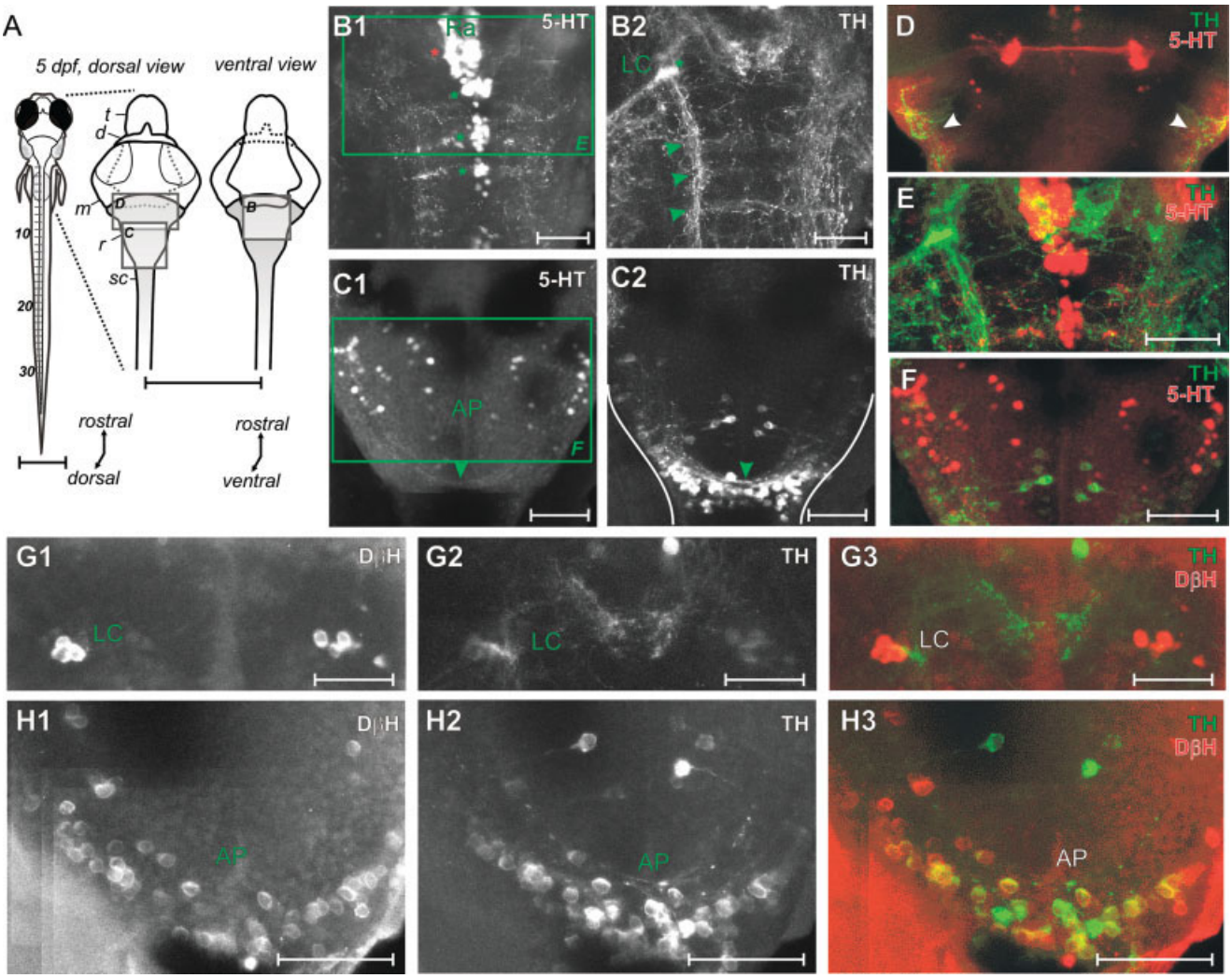

Fig. 7. Amine immunoreactivity in the rhombencephalon at 5 dpf; whole-mount dorsal and ventral view. **A:** Schematic drawings of a zebrafish larva (left panel), the whole-mount nervous system from the dorsal perspective (middle panel), and ventral perspective (right panel) that illustrate the regions depicted in B–D. For more details, see Figure 2. Arrows indicate orientation. **B:** Photo montages derived from collapsed optical sections (75 μm) illustrate 5-HT (B1) and TH (B2) reactivity in the ventral region of the rostral rhombencephalon. Red and green asterisks in B1 indicate the rhombomeric clustering of raphe (Ra) neurons. A green asterisk in B2 indicates the position of the locus coeruleus (LC). Green arrowheads indicate the segmental distribution of TH reactivity and the longitudinal tracts. **C:** Photo montages derived from collapsed optical sections (65 μm) illustrate 5-HT (C1) and TH (C2) reactivity in the dorsal region of the caudal rhombencephalon, near the area postrema (AP). Green arrowheads indicate faint commissural processes at the spinomedullary boundary. **D:** Collapsed optical sections (70 μm) illustrate 5-HT and TH reactivity in the cerebellar region (Ce). White arrowheads indicate regions that 5-HT and TH-reactive fibers ascend dorsally. **E:** Collapsed optical sections (75 μm) illustrate 5-HT and TH reactivity in the rostral raphe region, from the area marked by a green box in B1. **F:** Collapsed optical sections (65 μm) illustrate 5-HT and TH reactivity in the dorsal region of the caudal rhombencephalon, from the area marked by a green box in C1. **G:** Collapsed optical sections (60 μm) illustrate DβH (G1), TH (G2), and the resulting merge (G3) in the locus coeruleus. Note that although it is dimly labeled, TH and DβH reactivity always colocalize in the locus coeruleus. **H:** Collapsed optical sections (60 μm) illustrate DβH (H1), TH (H2), and the resulting merge (H3) in the dorsal region of the caudal rhombencephalon, near the area postrema. Note that TH and DβH reactivity do not always colocalize in this region. Scale bars = 0.5 mm in A; 50 μm in B1–H3.

unipolar process that projected ventrolaterally and then dorsally into the motor column (Fig. 8B3), where dendritic processes ramified and subsequently sent out an axonal process (see Fig. 9B2). Their axonal processes appeared to be descending and growth cones were often apparent after just 1–2 segments (Fig. 8D2). However, we should point out that due to the punctate nature of the immunoreactive labeling, we cannot rule out the possibility that a proportion of spinal 5-HT neurons may have longer descending processes. The pattern of dendritic arborization and short projection distance potentially distinguished these cells from ventromedial (VeMe) interneurons (Hale et al., 2001), which have dendrites located along the same horizontal plane as the soma and long, multisegmental descending processes.

To reveal the morphology of this serotonergic interneuron more clearly, we stochastically labeled neurons using green fluorescent protein (GFP). For this technique, a

DNA construct carrying GFP under the control of a pan-neuronal promoter is injected into one-cell-stage embryos. As development progresses, many cells lose the foreign DNA, but in those that retain the foreign DNA the expression of GFP occurs. The advantage of this technique is that only a limited number of cells are labeled very clearly, facilitating a detailed examination of their morphology, although we could not selectively drive expression into serotonergic neurons since we used the pan-neuronal promoter *HuC* (Park et al., 2000). When we screened genetically labeled fish for likely serotonergic interneuron candidates, we noted a neuron class whose cell body was located ventromedially, which had a characteristic curved process that projected into the ventrolateral cord and ramified, giving rise to a short, descending axonal process (Fig. 9A,B1-2). After immunocytochemical processing, we confirmed that this cell was indeed positive for 5-HT reactivity (Fig. 9C1-3). Furthermore, as an example from this same preparation illustrates, we also identified VeMe interneurons, due to their ventromedial location, long axonal process, and dendrites which extend along the same horizontal plane as the soma (Fig. 9D1). VeMe interneurons were not 5-HT-reactive (Fig. 9D2-3). Collectively, these findings confirm serotonergic spinal neurons as a distinct neuronal class.

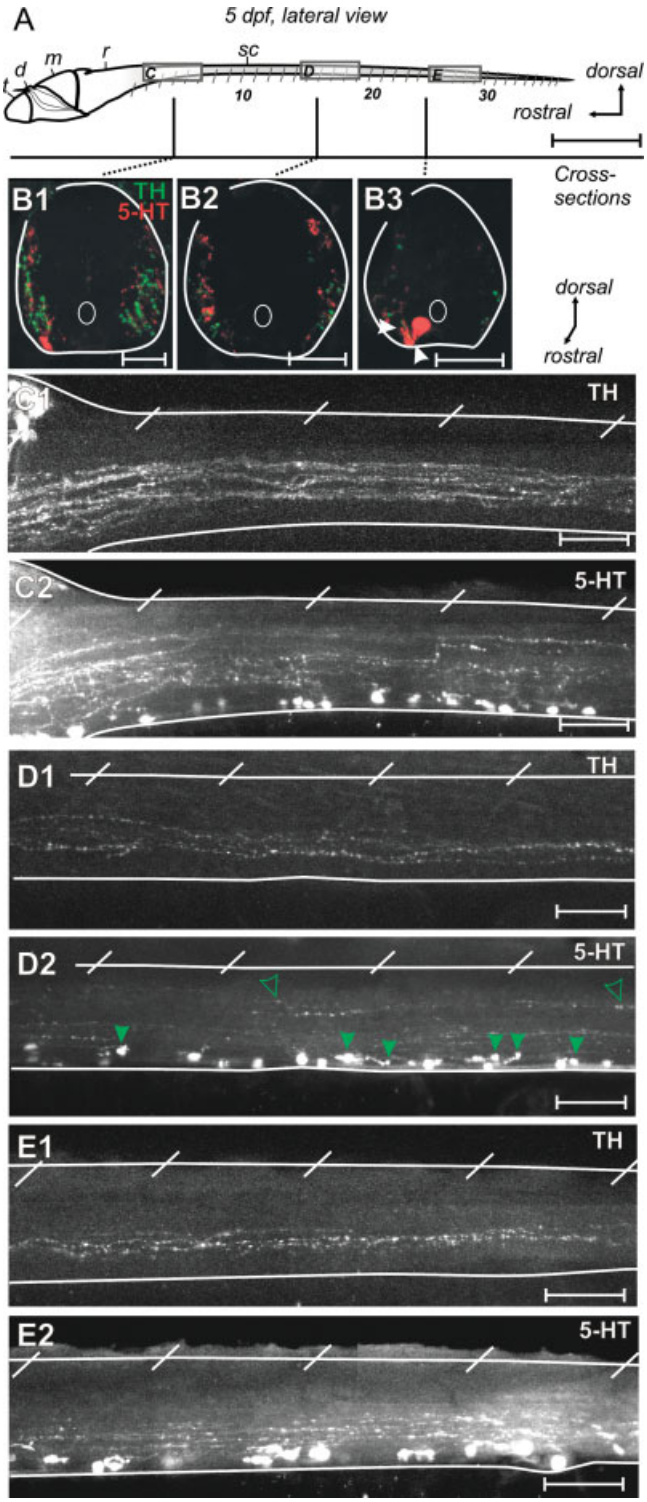

Ontogeny of aminergic immunofluorescence

The extensive amount of aminergic innervation at 5 dpf made it difficult to definitively determine the sources of fibers observed in the spinal cord. To help resolve this issue, we tracked the spatiotemporal expression of aminergic innervation up to 5 dpf, noting the emergence of aminergic populations and their processes. In the interest of brevity, our results for the temporal expression of amines in each brain structure have been tabulated (Fig. 10). In the following sections, we report the chronological pattern of spinal innervation.

Development from 0–4 dpf. The first TH-reactive neurons appeared between 16 and 24 hours postfertilization (hpf), in both the diencephalon and rhombencephalon (Fig. 11A,B). Already by this time, TH-reactive processes could be detected that passed the faint staining in the cells of the locus coeruleus on their way to the spinal cord, where growth cones were often apparent (Fig. 11B). Unfortunately, the presence of TH-reactive fibers as early as 24 hpf passing the locus coeruleus from the diencephalon obscured any possible descending fibers from the locus coeruleus. In close proximity to the diencephalic TH-

Fig. 8. Amine immunoreactivity in the spinal cord at 5 dpf; cross-section and whole-mount lateral view. **A:** A schematic drawing of the whole-mount nervous system that illustrates the regions depicted B–E. Arrows indicate orientation. **B:** TH and 5-HT in cross-section of the spinal cord from regions indicated in A. In the rostral spinal cord TH reactivity is predominantly located ventrally, although occasionally is detected dorsally, while 5-HT reactivity can be readily detected both ventrally and dorsally (B1). This is also true more than half-way down the spinal cord (B2). In the caudalmost segments TH and 5-HT reactivity are largely restricted to ventrolateral regions (B3). Note that the intraspinal 5-HT cell in B3 is located ventromedially, close to the central canal (white circle), with a characteristic curved process extending first ventrally and then dorsally into the motor column (at white arrowheads). **C:** Photo montages derived from collapsed optical sections (50 μm) illustrate TH (C1) and 5-HT (C2) reactivity at the spinomedullary boundary. In this and subsequent figures depicting the whole-mount spinal cord, slanted white lines indicate intermyotomal divisions. **D:** Collapsed optical sections (40 μm) illustrate TH (D1) and 5-HT (D2) reactivity from mid spinal cord. Open green arrowheads indicate the continuance of dorsally located 5-HT projections. Closed arrowheads mark growth cones. **E:** Collapsed optical sections (50 μm) illustrate TH (E1) and 5-HT (E2) reactivity from caudal spinal cord. Scale bars = 0.5 mm in A; 20 μm in B1–E2.

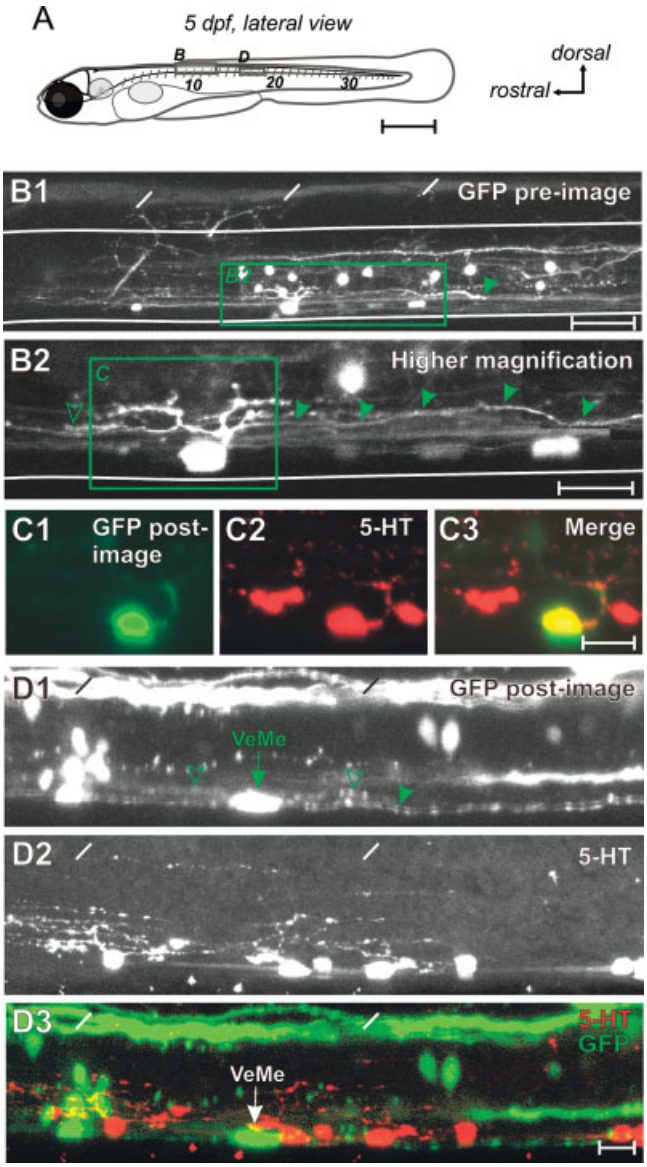

Fig. 9. Morphology of serotonergic cells in the spinal cord. **A:** A schematic drawing of a zebrafish larva that illustrates the regions depicted in B and D. For more details, see Figure 1 legend. Arrows indicate orientation. **B:** Photo montages derived from collapsed optical sections (40 μm, B1; 15 μm, B2) illustrate a serotonergic interneuron stochastically labeled with green fluorescent protein (GFP) using the HuC promoter (see Materials and Methods) in a living 5-day-old larva (preimage). Green arrowhead in B1 indicates the growth cone of the serotonergic interneuron. Green arrowheads in B2 indicate the descending process of the cell, while an open green arrowhead indicates a region of overlap with the rostralmost extent of the dendritic arborization of this cell and a more ventral descending process from another rostrally labeled cell. Note that the process from the serotonergic neuron only descends for a few muscle segments in B1. **C:** Collapsed optical sections (25 μm) of the same GFP labeled cell (C1, post-image) indicated in B after immunofluorescence processing for 5-HT (C2) illustrate that the cell is positive for 5-HT (C3). **D:** Collapsed optical sections (20 μm) from the same larva after immunofluorescence processing (post-image) illustrate a VeMe cell (D1, post-image), which is clearly not 5-HT-reactive (D2-3). Open green arrowheads indicate the dendritic processes of the VeMe cell which are slightly out of focus, while a green arrowhead marks the fuzzy axonal process, which was clearly identifiable originating from the soma in optical section. The projection patterns of the VeMe dendrites and axon markedly contrast those of the serotonergic interneuron. Scale bars = 0.5 mm in A; 50 μm in B1; 20 μm in B2; 10 μm in C, D.

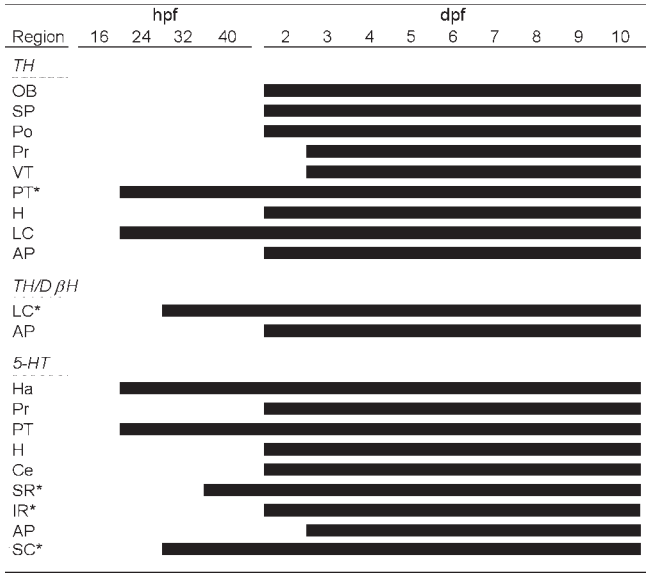

Fig. 10. Summary of aminergic neutron spatiotemporal appearance. *, indicates likely source of spinal innervatio. Abbreviations are based on anatomical terminology used in larval and adult zebrafish, see Discussion and abbreviation list for details.

reactive cells were 5-HT-reactive cells; however, there were no caudally projecting axons apparent from this population (Fig. 11C1-3). Even by this early stage, the morphology, location, and proximity of these diencephalic neurons to one another made them identifiable as the large pear-shaped cells of the posterior tuberculum and the arrowhead population, respectively. By 2 dpf (Fig. 12A), the large TH-reactive neurons were clearly distinguishable among the other TH-reactive neurons in the posterior tuberculum (Fig. 12D2). TH-reactive fibers could also be found in the ventrolateral margins of the mesencephalon (Fig. 12E2) and passing the locus coeruleus in the rhombencephalon (Fig. 12B2,F2) on their way to the spinal cord (Fig. 12G2,H2). By this stage, TH-reactive fibers in the ventrolateral cord (Fig. 12I2) could be detected along almost its entire length (Fig. 12C2).

By 32 hpf, 5-HT reactivity was detectable in cells within the spinal cord and by 2 dpf they had differentiated sufficiently to distinguish faint, short projecting processes (Fig. 12C1) in the ventrolateral cord (Fig. 12I1). Even by this stage there were no clear descending processes emerging from the serotonergic arrowhead population (Fig. 12D1,E1). Serotonergic reactivity was also detectable in the rostral raphe region, adjacent to the locus coeruleus (Fig. 12F1). These raphe cells had faint lateral processes that descended only to the level of the otic capsule (Fig. 12B1,G1,H1). Between 2–3 dpf, we noted rostral projections from these rostral raphe cells (data not illustrated) and the appearance of serotonergic cells more caudally, along the ventral midline (Fig. 12B1). By 3 dpf (Fig. 13A), we could observe 5-HT fibers in both dorsal and ventral locations in the rostral spinal cord (Fig. 13B1), with the dorsal processes reaching as far as the 10th–15th (Fig. 13C1) myotomal segment, where TH reactivity originating from the brain was already present (Fig. 13B2,C2). Unfortunately, because of the developmental appearance of both rostral and caudal raphe cells, we could not definitively

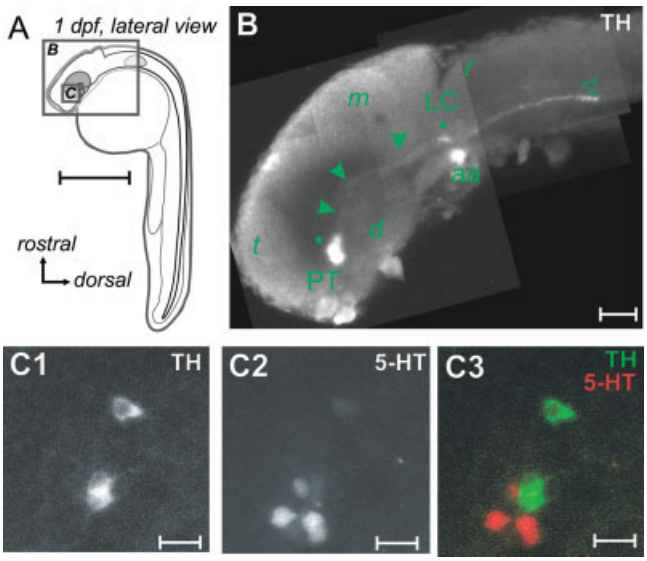

Fig. 11. Amine immunoreactivity at 1 dpf; whole-mount lateral view. **A:** A schematic drawing of a zebrafish embryo that illustrates the regions depicted in B, C. Arrows indicate orientation. **B:** A photo montage derived from collapsed optical sections (100 μm, left portion of composite; 40 μm right portion of composite) illustrates TH reactivity from the region indicated in A. Even at this early stage the telencephalon (t), diencephalon (d), mesencephalon (m), and rhombencephalon (r) can be distinguished. Green arrowheads indicate descending TH fibers from the posterior tuberculum (PT). An open green arrowhead indicates a growth cone at the end of these fibers. Green asterisks mark TH reactivity in the posterior tuberculum and the locus coeruleus (LC). Also obvious is the intense labeling in the arch-associated neurons (aa). Scale bar = 50 μm. **C:** Collapsed optical sections (60 μm) illustrate TH (C1), 5-HT (C2), and the resulting merge (C3) from the ventral diencephalon of a different preparation. Scale bars = 0.5 mm in A; 20 μm in B–C.

distinguish from which source the dorsal 5-HT-reactive fibers in the spinal cord derived. Also, due to the concomitant timing of descending 5-HT fibers from the raphe region and fibers from the spinal 5-HT cells, it was difficult to establish whether processes from the raphe also innervated ventral spinal cord. Regardless, it seemed clear that a proportion of spinal 5-HT innervation was raphespinal in origin. The spinal 5-HT cells had differentiated sufficiently by 3 dpf to see short projecting axons derived from the dendritic arbor, with rather large growth cones (Fig. 13B1). By 4 dpf, the pattern of spinal aminergic innervation described above at 5 dpf was in place. Based on this spatiotemporal description of aminergic populations, there were three likely candidates for the aminergic innervation of spinal cord from the brain: 1) the large cells in the posterior tuberculum (DA); 2) the cells of the locus coeruleus (NA); and 3) the cells in the raphe region (5-HT).

Thus, by 4–5 days when larva are freely swimming in the water column there is already a considerable amount of aminergic innervation of the nervous system, particularly within the spinal cord. However, we were concerned about how stable the pattern of reactivity observed at 5 dpf was. For functional experiments, it would be useful to know if larvae older than 5 dpf could be treated equally with respect to aminergic innervation. Therefore, we continued to track the patterns of aminergic reactivity up to 10 dpf.

Development from 6–10 dpf. Between 6–10 dpf, no new populations emerged that expressed TH, 5-HT, or DβH immunoreactivity (Fig. 10). By 10 dpf, the three most likely aminergic candidates for descending spinal innervation were still present and did not appear to increase in population size. To confirm this, we performed cell counts of each population at 5 and 10 dpf. In the posterior tuberculum, at 5 dpf there were ~15 large cells per side on average (14.9 ± 0.6; n = 5), which did not dramatically increase by 10 dpf (15.9 ± 0.6; n = 5). Similarly, in the locus coeruleus there were around 5 cells per side both at 5 dpf (4.8 ± 0.3; n = 5) and 10 dpf (5.3 ± 0.3; n = 5). Because the rostral and caudal regions of the raphe represented such a large population combined, we limited our cell counts to only the rostral raphe region for the purposes of comparison. The large cells of the rostral raphe region numbered about 25 cells per side at 5 dpf (24.7 ± 2.3; n = 5) and did not increase substantially by 10 dpf (25.3 ± 0.7; n = 5). Of course, on the basis of evidence presented here, we cannot ascertain exactly what proportion of these populations actually projects to spinal cord (see, however, following article).

Consistent with the lack of change in population number, by 10 dpf (Fig. 14A) there was no noticeable increase in the amount of aminergic innervation or changes in the regions innervated. For example, descending TH-reactive processes originating from the posterior tuberculum were obvious (Fig. 14B1), and so too were TH and 5-HT-reactive fibers in the lateral and ventral aspects of the rhombencephalon (Fig. 14B1-2,C1-2). In addition, there was still a marked amount of TH- and 5-HT-reactive fibers in the dorsal rhombencephalon, cerebellum, and at the level of the otic capsule (Fig. 14C1-2). Most important, the extent of spinal aminergic innervation remained the same (Fig. 14D1-2), with TH reactivity restricted predominantly to the ventrolateral aspects of the spinal cord and 5-HT reactivity in both dorsal and ventral regions (Fig. 14E1-3). Also as at 5 dpf, in the caudalmost regions of the spinal cord aminergic fibers could only be found ventrally, along with spinal 5-HT cells (Fig. 14F1-2). Therefore, even by 10 dpf there were no obvious changes in the patterns of aminergic innervation.

DISCUSSION

We have described the pattern of aminergic innervation from 0–10 dpf. Our study expands on previous ones by detailing the putative interrelationship of three aminergic populations and the course of their fiber tracts and commissures throughout the nervous system. The pattern of spinal aminergic innervation by 4–5 dpf does not change noticeably up to 10 dpf. Therefore, the descending amines in zebrafish might contribute to their rapid behavioral transition from hatching to hunting.

Methodological considerations

We used immunochemicals and procedures already applied in adult zebrafish (Kaslin and Panula, 2001). As in adults, these immunoreagents derived from mammalian sources reliably labeled specific structures within the nervous system of embryos and larvae, making it likely that they are recognizing zebrafish equivalents of TH, 5-HT, and DβH. Our pattern of reactivity matched that described in adult zebrafish (Kaslin and Panula, 2001; Rink and Wullimann, 2001), with the notable exception of DβH

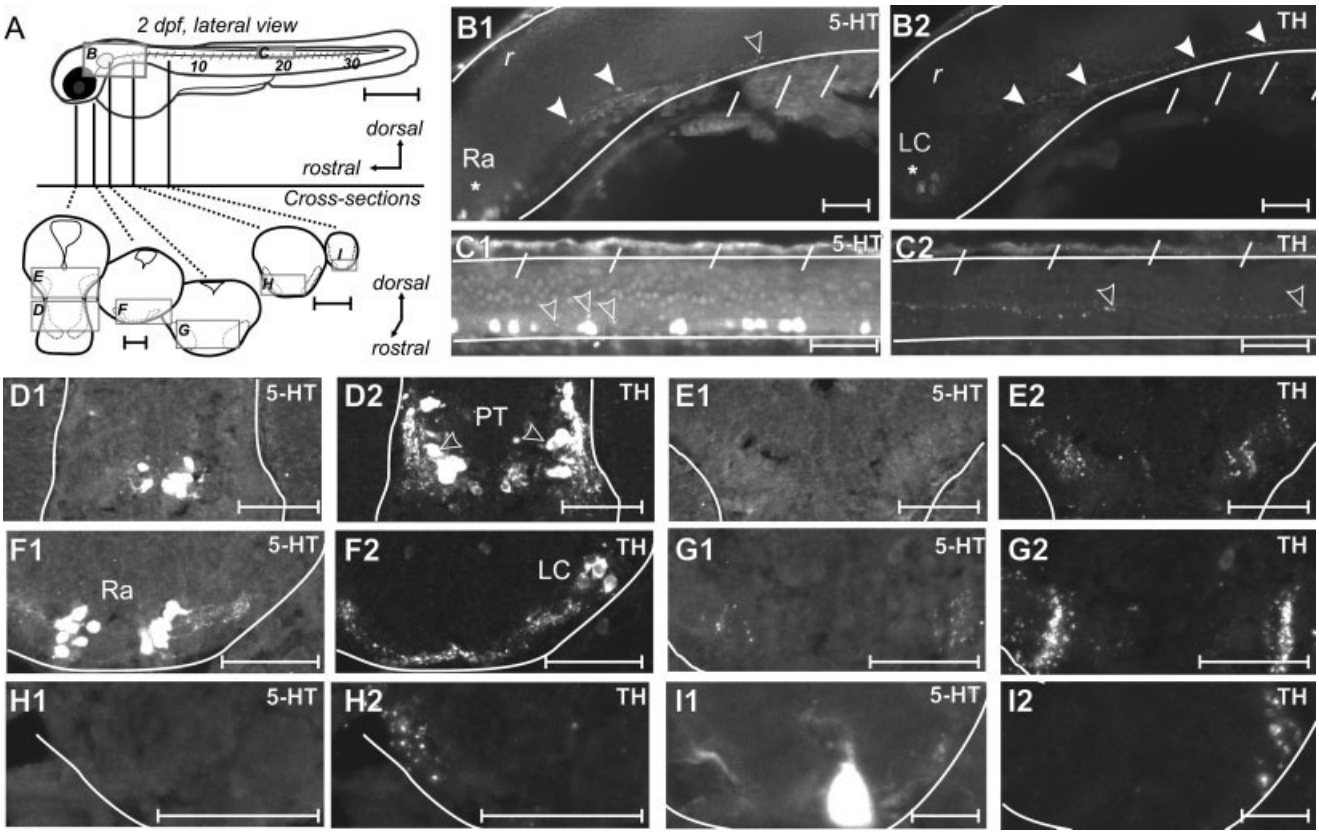

Fig. 12. Amine immunoreactivity at 2 dpf: cross-section and whole-mount lateral view. **A:** A schematic drawing of a zebrafish embryo that illustrates the regions depicted in B–I. Arrows indicate orientation. **B:** Photo montages derived from collapsed optical sections (60 μm) illustrate 5-HT (B1) and TH (B2) reactivity in the rhombencephalon (r). White arrowheads indicate descending TH and 5-HT-reactive fibers, while an open white arrowhead shows where the 5-HT reactivity stops, well short of the spinal cord. White asterisks mark the rostral raphe (Ra) region and the locus coeruleus (LC). Note that both TH and 5-HT-reactive fibers appear to begin at the level of the otic capsule due to their emergence from more medial regions at that location. Note also the appearance of the smaller, caudal raphe cells in this region. **C:** Collapsed optical sections (40 μm) illustrate 5-HT (C1) and TH (C2) reactivity in the spinal cord. Open white arrowheads indicate the faint, punctate ventral 5-HT- and TH-reactive fibers. **D:** A cross-section image illustrates 5-HT (D1) and TH (D2) reactivity in the ventral diencephalon. Open white arrowheads mark two of the larger cells in the posterior tuberculum (PT). **E:** A cross-section image illustrates 5-HT (E1) and TH (E2) reactivity in the ventral mesencephalon. Note the presence of TH-reactive processes, but the absence of 5-HT-reactive ones. **F:** A cross-section image illustrates 5-HT (F1) and TH (F2) reactivity in the rostral rhombencephalon. Here neurons from the rostral raphe region and locus coeruleus are obvious, as are sites where their projections overlap. **G:** A cross-section illustrates 5-HT (G1) and TH reactivity (G2) in the mid-rostral rhombencephalon. Note descending processes from the raphe, posterior tuberculum, and, possibly, the locus coeruleus are present ventrolaterally. **H:** A cross-section illustrates 5-HT (H1) and TH (H2) reactivity in the caudal rhombencephalon. Note the absence of 5-HT reactivity. **I:** A cross-section illustrates 5-HT (I1) and TH (I2) reactivity in the rostral spinal cord. Here 5-HT and TH reactivity in the ventrolateral cord are obvious, as is a process that extends dorsally from the soma of a spinal 5-HT neuron. Scale bars = 0.5 mm in A (top); 50 μm L–I (cross-sections), B1–H2; 10 μm in I1, I2.

staining. In adults, DβH reactivity was detected throughout noradrenergic neurons, within the cell body and accompanying processes (Kaslin and Panula, 2001). In our hands, DβH reactivity using identical reagents was restricted to the soma and initial axon segment. We are unsure why this was the case. The synthesis of NA from DA by DβH occurs within synaptic vesicles (Iversen et al., 1980). One potential explanation could be that the antibody directed to DβH did not have sufficient access to DβH once it was incorporated into vesicles and trafficked to the peripheral structures of the cell. Alternatively, it could be that these sites of release were sufficiently small and punctate at this developmental stage that they were difficult to see. Because DβH staining did not label noradrenergic processes, we cannot rule out the possibility that the locus coeruleus may contribute to some of the TH reactivity observed in the spinal cord.

Projection patterns of larval aminergic neurons: comparisons with adult zebrafish

There are many parallels between larval and adult aminergic systems. Both have TH-reactive cells in the olfactory bulb. These probably only project locally in larvae, as they do locally within the primary olfactory layer and glomerular layer of adults (Byrd and Brunjes, 1995; Kaslin and Panula, 2001). Regions just caudal to the olfactory bulb in adults are accessed by aminergic systems via the longitudinal catecholamine bundle, which runs contiguously from the spinomedullary junction via the mesencephalon and diencephalon, into the telencephalon

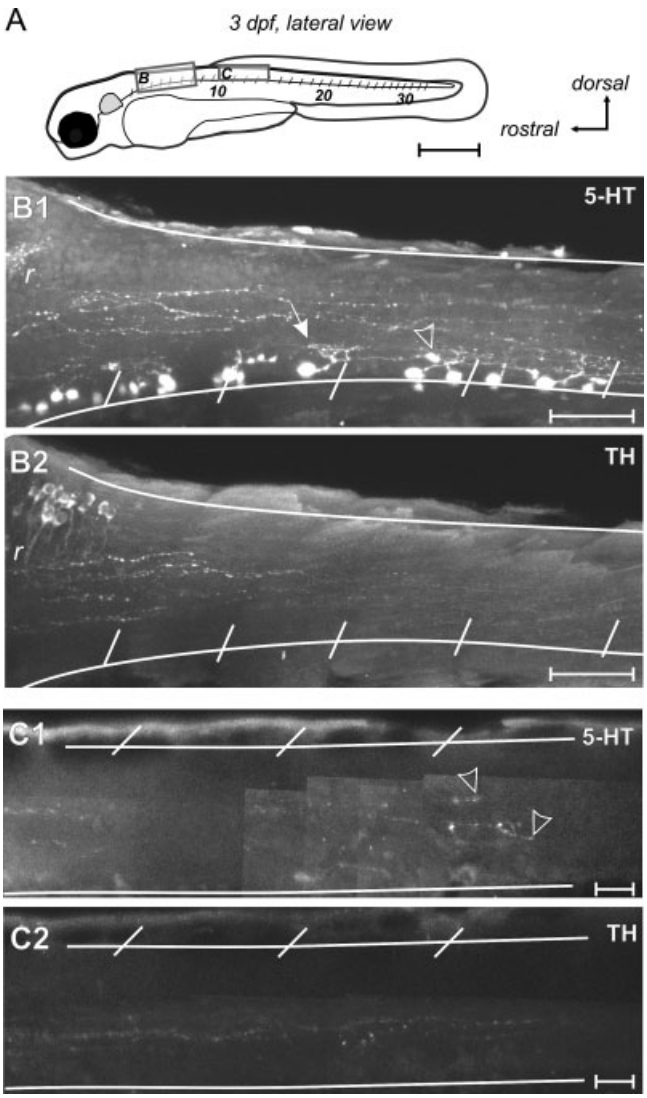

Fig. 13. Amine immunoreactivity at 3 dpf: whole-mount lateral view. **A:** A schematic drawing of a zebrafish embryo that illustrates the regions depicted in B, C. Arrows indicate orientation. **B:** Photo montages derived from collapsed optical sections (60 μm) illustrate 5-HT (B1) and TH (B2) reactivity at the spinomedullary border. A white arrow indicates the dendritic arborizations of a spinal 5-HT neuron, while an open white arrowhead illustrates a growth cone at the end of its short descending process. Scale bars = 50 μm. **C:** Collapsed optical sections (65 μm) illustrate faint 5-HT (C1) and TH (C2) reactivity in the mid-spinal cord. Open white arrowheads indicate growth cones and thus the extent that dorsal fibers project down the spinal cord by this developmental stage. Scale bars = 0.5 mm in A; 20 μm in B1–C2.

(Ma, 1994b). Populations that are thought to contribute to telencephalic aminergic innervation include the preoptic region and the locus coeruleus (Ma, 1994b; Rink and Wullimann, 2001; Ma, 2003). The preoptic group is defined in adults as the preoptic nuclear complex and consists of a number of different subclasses, which primarily project via the preoptico-hypophyseal dopaminergic tract (PHT) into the caudal reaches of the hypothalamus (Ma, 2003). Even at the early stages we studied, different neurons within the preoptic region appear to be distinguishable, possibly relating to different functions, as in adults (Ma, 2003). The pretectal group of TH-reactive cells is reported in adults to project within the pretectal region, ventrally into the dorsal thalamus, and dorsally into the dorsomedial optic tectum (Ma, 2003), which is consistent with our observations from larvae. Similarly, the population of TH-reactive cells in the ventral thalamus in adults only projects to the lateral edge of the diencephalon, where they ramify weakly (Ma, 2003), as they appear to do in larvae.

The large, pear-shaped neurons we observed most likely correspond to those termed either the periventricular organ-accompanying cells (PVOa) (Ma, 2003), the periventricular nucleus of the posterior tuberculum (TPp) (Becker et al., 1997), or posterior tuberal nucleus (PTN) (Kaslin and Panula, 2001). These rather large cells have substantial primary and secondary dendrites, off of which extensive arbors and long projecting axons derive (Ma, 2003). Their projections extend as far rostral as the postoptic commissure, arborize extensively within the ventral hypothalamus and posterior tubercular area by way of tracts within the diencephalon, including the PHT and endohypothalamic tract (EHT) (Ma, 2003). They also project dorsally, then caudally following the medial longitudinal fascicle into the medulla, where they innervate the cerebellum and continue on into the spinal cord (Becker et al., 1997; Ma, 2003). Again, we found neurons fitting this description in larval zebrafish, which we believe innervate the spinal cord.

Overlapping these large cells is a population of TH-reactive cells identified in adult zebrafish as the dorsomedial cell group of the caudal zone of the periventricular hypothalamus, or Hc(dm) (Ma, 2003). These neurons are characterized by a rostrocaudal orientation of cell bodies and a primary process that first projects rostrally, then either proceeds out from the caudal hypothalamus into the isthmus or projects locally within the hypothalamus, contributing to the EHT (Ma, 2003). This population bears a striking similarity to the one we have described overlapping the larger posterior tuberculum cells. In addition, scattered throughout the diencephalon in adults are TH-reactive cells that contact cerebrospinal fluid and only project very locally (Ma, 2003), similar to the ones we described in larvae.

The locus coeruleus is defined as noradrenergic by its coexpression of TH and DβH reactivity. In adults, it innervates more rostral structures via two aminergic pathways, the longitudinal catecholamine bundle and the periventricular catecholamine pathway (Ma, 1994b). In addition, neurons from the locus coeruleus are known to innervate the raphe nucleus and also send a small proportion of their axons caudally, perhaps even into the spinal cord (Ma, 1994b). This is consistent with our observations from larvae.

The final population of catecholaminergic neurons in the caudal medulla consists of three distinguishable subpopulations in adults: an interfascicular group ($infas_{CA}$), a vagal group ($vagal_{CA}$), and an area postrema group ($apost_{CA}$) (Ma, 1997). While all three groups have relatively local projections, are comprised of dopaminergic and noradrenergic neurons, and contribute to the longitudinal catecholamine bundle within the medulla, each also has distinguishing characteristics (Ma, 1997). For instance, the $infas_{CA}$ neurons are located more rostrally, have commissural processes, and are morphologically very similar

to the locus coeruleus neurons, leading to their suggested identity as segmental homologs (Ma, 1997). The $vagal_{CA}$ group has a similar morphology to the $infas_{CA}$ group and is contiguous with the $apost_{CA}$ groups (Ma, 1997). The $infas_{CA}$ and $vagal_{CA}$ groups could correspond to the more rostral and medial contingent, respectively, of the caudal medullary population described here. The $apost_{CA}$, the caudalmost group located at the medullospinal border, contains both dopaminergic and noradrenergic neurons which are densely packed in a horseshoe shape when observed in horizontal section (Ma, 1997). Similar neurons were observed here in larval zebrafish at the caudalmost extent of the spinomedullary boundary. The subdivisions of these medullary catecholaminergic groups thus appear to arise early in development.

While the pattern of 5-HT-reactive cells and fibers has been described in adult zebrafish (Kaslin and Panula, 2001), there is no description of the precise targets of these populations. We can, however, infer the likely targets based on our own data. The earliest differentiating population of 5-HT cells originated in the diencephalon and the projections from these cells appeared to terminate locally. This is consistent with the projection patterns of TH-reactive cells in the diencephalon with similar morphology. It is likely that our distinction of larger, rostral raphe neurons and smaller, caudal raphe neurons correspond to the superior and inferior raphe, respectively, as described in adult zebrafish (Wullimann et al., 1996; Kaslin and Panula, 2001). Indeed, the raphe region is known to project to spinal cord in adult salmon, goldfish, and zebrafish, which is consistent with our findings (Oka et al., 1986; Prasada Rao et al., 1993; Becker et al., 1997). We also observed ascending processes from the larger, rostral (superior) raphe neurons, indicating they contribute to the 5-HT reactivity found in more rostral brain regions. Their descending processes are also potentially a source of the segmentally distributed 5-HT reactivity observed in the medulla. However, the segmental distribution of the smaller, caudal (inferior) raphe cells, and the coincidence of their time of origin with the appearance of the punctate, segmental labeling, suggests that these smaller 5-HT cells could also contribute to the intramedullary, segmental 5-HT innervation. The later developmental appearance of the pretectal and caudal medullary serotonergic populations (Fig. 10) make determinations of their targets more difficult. It could be that their similar location and morphology to the TH-reactive neurons in the same regions indicate a similar projection profile. If this is the case, then the pretectal 5-HT cells will innervate the optic tectum, while the caudal medullary 5-HT cells will contribute

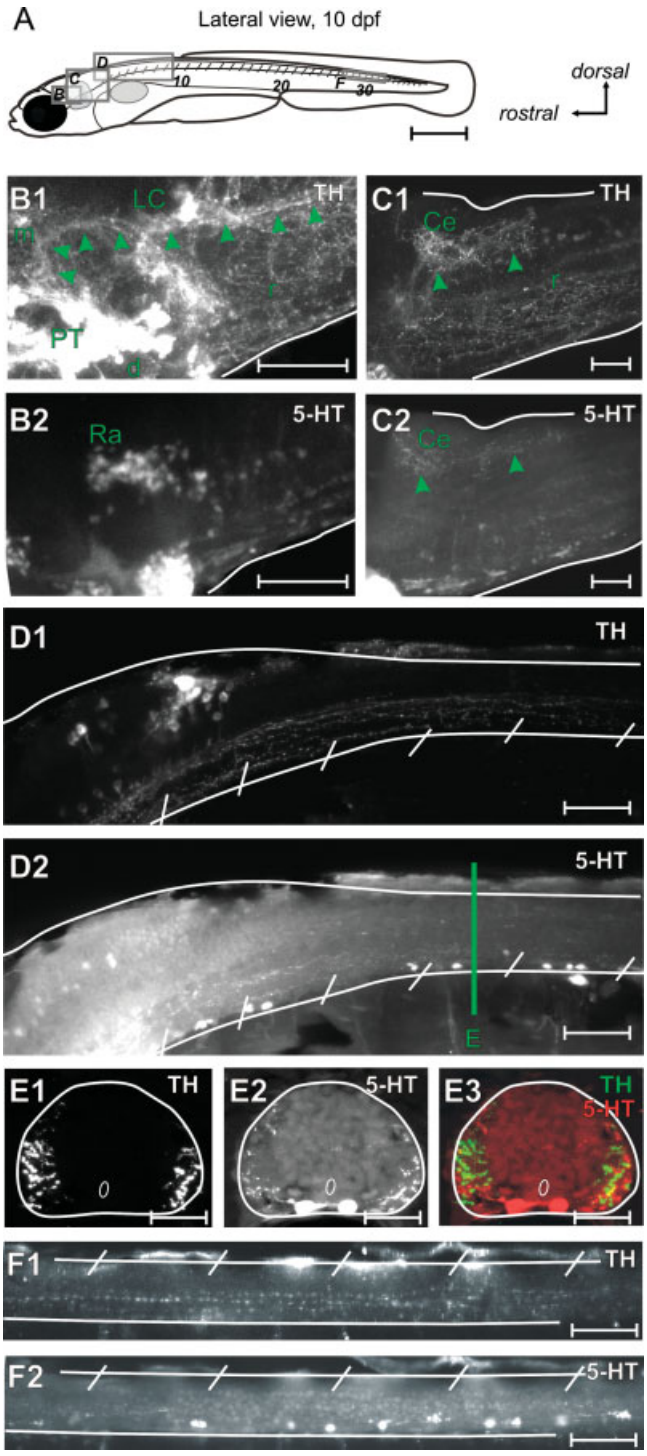

Fig. 14. Amine immunoreactivity at 10 dpf; whole-mount lateral view. **A:** A schematic drawing of a zebrafish larva illustrates the regions depicted in B–E. Arrows indicate orientation. **B:** Photo montages derived from collapsed optical sections (40 μm) illustrate TH (B1) and 5-HT (B2) reactivity at the border between the diencephalon (d), mesencephalon (m), and rhombencephalon (r). Green arrowheads mark the tract of TH reactivity that originates from the posterior tuberculum (PT) and passes the locus coeruleus (LC) on its way to the spinal cord. Note the large raphe neurons (Ra) located in the same region as the locus coeruleus. **C:** Collapsed optical sections (130 μm) illustrate TH (C1) and 5-HT (C2) reactivity in the rostral rhombencephalon. Green arrowheads indicate the TH and 5-HT-reactive fibers that innervate the dorsal rhombencephalon and cerebellum (Ce). **D:** Collapsed optical sections (30 μm) illustrate TH (D1) and faint, punctate 5-HT (D2) reactivity at the border of the rhombencephalon and spinal cord. **E:** A cross-section of TH (F1), 5-HT (F2), and the resulting merge (F3) in the rostral spinal cord, as indicated in D2. **F:** Collapsed optical sections (15 μm) illustrate TH (E1) and 5-HT (E2) reactivity in the caudal spinal cord. Note that at 10 dpf dorsal 5-HT-reactive fibers are not detected in the caudalmost reaches of the spinal cord as in 5 dpf larva. Scale bars = 0.5 mm in A; 50 μm in B–D, F; 20 μm in E.

to serotonergic innervation observed in more rostral brain regions.

CONCLUSIONS

In summary, the overall pattern of nuclei and tracts in larval fish corresponds well with the aminergic populations and tracts described by others in adult zebrafish. Embryonic pathways may be completely replaced during development or merely enlarge and migrate to their more central positions (Wullimann et al., 1996). The good topological correspondence between embryonic and at least some adult tracts and commissures, combined with our results placing aminergic neurons in brain regions described in adults, suggest the latter. Strikingly, the cell numbers reported here for the putative dopaminergic and noradrenergic sources of spinal innervation are in agreement with those reported in adult fish (Ma, 1994a; Ma and Lopez, 2003). Thus, the early pattern of aminergic innervation appears to form a framework upon which the adult pattern of reactivity is based. If so, these regions are likely to be functional in a behavioral context early in life, where they may regulate sensorimotor processing in the brain (discussed in Ma, 1994a,b, 1997, 2003; Kaslin and Panula, 2001) and spinal cord (see following article). This would not be completely surprising, since by 4–5 days larval zebrafish are a fully functioning organism in their own right, interacting with their environment as efficient hunters (Kimmel et al., 1974; Fuiman and Webb, 1988; Budick and O'Malley, 2000; Borla et al., 2002). These aminergic systems are established at a time when zebrafish are amenable to optical, genetic, and electrophysiological approaches to reveal the links between neuronal circuits and behavior (Fetcho, 2001; Drapeau et al., 2002; O'Malley et al., 2003). Our data provide a morphological foundation for using these tools to explore the functional organization of aminergic systems and their contributions to axial motor behavior.

ACKNOWLEDGMENTS

We thank S. Higashijima for invaluable discussions and for generating the genetically labeled fish used in this study; D. Bhatt and M. Masino for critically reading early versions of the article; and R. Grady, M. Lamendola, and H. Patzelova for excellent technical support and fish care.

LITERATURE CITED

Ali DW, Drapeau P, Legendre P. 2000. Development of spontaneous glycinergic currents in the Mauthner neuron of the zebrafish embryo. J Neurophysiol 84:1726–1736.

Becker T, Wullimann MF, Becker CG, Bernhardt RR, Schachner M. 1997. Axonal regrowth after spinal cord transection in adult zebrafish. J Comp Neurol 377:577–595.

Bellipanni G, Rink E, Bally-Cuif L. 2002. Cloning of two tryptophan hydroxylase genes expressed in the diencephalon of the developing zebrafish brain. Gene Expr Patterns 2:251–256.

Bernhardt RR, Chitnis AB, Lindamer L, Kuwada JY. 1990. Identification of spinal neurons in the embryonic and larval zebrafish. J Comp Neurol 302:603–616.

Borla MA, Palecek B, Budick S, O'Malley DM. 2002. Prey capture by larval zebrafish: evidence for fine axial motor control. Brain Behav Evol 60:207–229.

Budick SA, O'Malley DM. 2000. Locomotor repertoire of the larval zebrafish: swimming, turning and prey capture. J Exp Biol 203:2565–2579.

Byrd CA, Brunjes PC. 1995. Organization of the olfactory system in the adult zebrafish: histological, immunohistochemical, and quantitative analysis. J Comp Neurol 358:247–259.

Cazalets JR, Grillner P, Menard I, Cremieux J, Clarac F. 1990. Two types of motor rhythm induced by NMDA and amines in an in vitro spinal cord preparation of neonatal rat. Neurosci Lett 111:116–121.

Cazalets JR, Gardette M, Hilaire G. 2000. Locomotor network maturation is transiently delayed in the MAOA-deficient mouse. J Neurophysiol 83:2468–2470.

Cowley KC, Schmidt BJ. 1994. A comparison of motor patterns induced by N-methyl-D-aspartate, acetylcholine and serotonin in the in vitro neonatal rat spinal cord. Neurosci Lett 171:147–150.

Drapeau P, Ali DW, Buss RR, Saint-Amant L. 1999. In vivo recording from identifiable neurons of the locomotor network in the developing zebrafish. J Neurosci Methods 88:1–13.

Drapeau P, Saint-Amant L, Buss RR, Chong M, McDearmid JR, Brustein E. 2002. Development of the locomotor network in zebrafish. Prog Neurobiol 68:85–111.

Fetcho JR. 2001. Optical and genetic approaches toward understanding spinal circuits. In: Cope TC, editor. Motor neurobiology of the spinal cord. New York: CRC Press. p 3–20.

Fetcho JR, O'Malley DM. 1995. Visualization of active neural circuitry in the spinal cord of intact zebrafish. J Neurophysiol 73:399–406.

Fuiman LA, Webb PW. 1988. Ontogeny of routine swimming activity and performance in zebra Danios (Teleostei, Cyprinidae). Anim Behav 36: 250–261.

Gahtan E, O'Malley DM. 2003. Visually guided injection of identified reticulospinal neurons in zebrafish: a survey of spinal arborization patterns. J Comp Neurol 459:186–200.

Gahtan E, Sankrithi N, Campos JB, O'Malley DM. 2002. Evidence for a widespread brain stem escape network in larval zebrafish. J Neurophysiol 87:608–614.

Gleason MR, Higashijima S, Dallman J, Liu K, Mandel G, Fetcho JR. 2003. Translocation of CaM kinase II to synaptic sites in vivo. Nat Neurosci 6:217–218.

Grillner S. 1985. Neurobiological bases of rhythmic motor acts in vertebrates. Science 228:143–149.

Grillner S, Wallén P. 2002. Cellular bases of a vertebrate locomotor system-steering, intersegmental and segmental co-ordination and sensory control. Brain Res Rev 40:92–106.

Guo S, Brush J, Teraoka H, Goddard A, Wilson SW, Mullins MC, Rosenthal A. 1999. Development of noradrenergic neurons in the zebrafish hindbrain requires BMP, FGF8, and the homeodomain protein soulless/Phox2a. Neuron 24:555–566.

Guo S, Yamaguchi Y, Schilbach S, Wada T, Lee J, Goddard A, French D, Handa H, Rosenthal A. 2000. A regulator of transcriptional elongation controls vertebrate neuronal development. Nature 408:366–369.

Hale ME, Ritter DA, Fetcho JR. 2001. A confocal study of spinal interneurons in living larval zebrafish. J Comp Neurol 437:1–16.

Higashijima S, Okamoto H, Ueno N, Hotta Y, Eguchi G. 1997. High-frequency generation of transgenic zebrafish which reliably express GFP in whole muscles or the whole body by using promoters of zebrafish origin. Dev Biol 192:289–299.

Higashijima S, Masino MA, Mandel G, Fetcho JR. 2003. Imaging neuronal activity during zebrafish behavior with a genetically encoded calcium indicator. J Neurophysiol 90:3986–3997.

Holzschuh J, Ryu S, Aberger F, Driever W. 2001. Dopamine transporter expression distinguishes dopaminergic neurons from other catecholaminergic neurons in the developing zebrafish embryo. Mech Dev 101:237–243.

Iizuka M, Nishimaru H, Kudo N. 1998. Development of the spatial pattern of 5-HT-induced locomotor rhythm in the lumbar spinal cord of rat fetuses in vitro. Neurosci Res 31:107–111.

Iversen LL, Lee CM, Gilbert RF, Hunt S, Emson PC. 1980. Regulation of neuropeptide release. Proc R Soc Lond B Biol Sci 210:91–111.

Kaslin J, Panula P. 2001. Comparative anatomy of the histaminergic and other aminergic systems in zebrafish (Danio rerio). J Comp Neurol 440:342–377.

Kiehn O, Butt SJ. 2003. Physiological, anatomical and genetic identification of CPG neurons in the developing mammalian spinal cord. Prog Neurobiol 70:347–361.

Kiehn O, Kjaerulff O. 1996. Spatiotemporal characteristics of 5-HT and dopamine-induced rhythmic hindlimb activity in the in vitro neonatal rat. J Neurophysiol 75:1472–1482.

Kiehn O, Sillar KT, Kjaerulff O, McDearmid JR. 1999. Effects of noradrenaline on locomotor rhythm-generating networks in the isolated neonatal rat spinal cord. J Neurophysiol 82:741–746.

Kimmel CB. 1982. Reticulospinal and vestibulospinal neurons in the young larva of a teleost fish, Brachydanio rerio. Prog Brain Res 57:1–23.

Kimmel CB, Patterson J, Kimmel RO. 1974. The development and behavioral characteristics of the startle response in the zebrafish. Developmental Psychobiology 7:47–60.

Kimmel CB, Ballard WW, Kimmel SR, Ullmann B, Schilling TF. 1995. Stages of embryonic development of the zebrafish. Dev Dyn 203:253–310.

Kudo N, Nishimaru H, Nakayama K. 2004. Developmental changes in rhythmic spinal neuronal activity in the rat fetus. Prog Brain Res 143:49–55.

Lakke EA. 1997. The projections to the spinal cord of the rat during development: a timetable of descent. Adv Anat Embryol Cell Biol 135:I-XIV, 1–143.

Liu KS, Fetcho JR. 1999. Laser ablations reveal functional relationships of segmental hindbrain neurons in zebrafish. Neuron 23:325–335.

Lorent K, Liu KS, Fetcho JR, Granato M. 2001. The zebrafish space cadet gene controls axonal pathfinding of neurons that modulate fast turning movements. Development 128:2131–2142.

Ma PM. 1994a. Catecholaminergic systems in the zebrafish. I. Number, morphology, and histochemical characteristics of neurons in the locus coeruleus. J Comp Neurol 344:242–255.

Ma PM. 1994b. Catecholaminergic systems in the zebrafish. II. Projection pathways and pattern of termination of the locus coeruleus. J Comp Neurol 344:256–269.

Ma PM. 1997. Catecholaminergic systems in the zebrafish. III. Organization and projection pattern of medullary dopaminergic and noradrenergic neurons. J Comp Neurol 381:411–427.

Ma PM. 2003. Catecholaminergic systems in the zebrafish. IV. Organization and projection pattern of dopaminergic neurons in the diencephalon. J Comp Neurol 460:13–37.

Ma PM, Lopez M. 2003. Consistency in the number of dopaminergic paraventricular organ-accompanying neurons in the posterior tuberculum of the zebrafish brain. Brain Res 967:267–272.

Metcalfe WK, Mendelson B, Kimmel CB. 1986. Segmental homologies among reticulospinal neurons in the hindbrain of the zebrafish larva. J Comp Neurol 251:147–159.

Norreel JC, Pflieger JF, Pearlstein E, Simeoni-Alias J, Clarac F, Vinay L. 2003. Reversible disorganization of the locomotor pattern after neonatal spinal cord transection in the rat. J Neurosci 23:1924–1932.

Oka Y, Satou M, Ueda K. 1986. Descending pathways to the spinal cord in the hime salmon (landlocked red salmon, Oncorhynchus nerka). J Comp Neurol 254:91–103.

O'Malley DM, Kao YH, Fetcho JR. 1996. Imaging the functional organization of zebrafish hindbrain segments during escape behaviors. Neuron 17:1145–1155.

O'Malley DM, Zhou Q, Gahtan E. 2003. Probing neural circuits in the zebrafish: a suite of optical techniques. Methods 30:49–63.

Park HC, Kim CH, Bae YK, Yeo SY, Kim SH, Hong SK, Shin J, Yoo KW, Hibi M, Hirano T, Miki N, Chitnis AB, Huh TL. 2000. Analysis of upstream elements in the HuC promoter leads to the establishment of transgenic zebrafish with fluorescent neurons. Dev Biol 227:279–293.

Pearson KG. 1993. Common principles of motor control in vertebrates and invertebrates. Annu Rev Neurosci 16:265–297.

Pflieger JF, Clarac F, Vinay L. 2002. Postural modifications and neuronal excitability changes induced by a short-term serotonin depletion during neonatal development in the rat. J Neurosci 22:5108–5117.

Prasada Rao PD, Jadhao AG, Sharma SC. 1993. Topographic organization of descending projection neurons to the spinal cord of the goldfish, Carassius auratus. Brain Res 620:211–220.

Rink E, Wullimann MF. 2001. The teleostean (zebrafish) dopaminergic system ascending to the subpallium (striatum) is located in the basal diencephalon (posterior tuberculum). Brain Res 889:316–330.

Rink E, Wullimann MF. 2002. Development of the catecholaminergic system in the early zebrafish brain: an immunohistochemical study. Dev Brain Res 137:89–100.

Ritter DA, Bhatt DH, Fetcho JR. 2001. In vivo imaging of zebrafish reveals differences in the spinal networks for escape and swimming movements. J Neurosci 21:8956–8965.

Schmidt BJ, Jordan LM. 2000. The role of serotonin in reflex modulation and locomotor rhythm production in the mammalian spinal cord. Brain Res Bull 53:689–710.

Sillar KT, Reith CA, McDearmid JR. 1998. Development and aminergic neuromodulation of a spinal locomotor network controlling swimming in Xenopus larvae. Ann N Y Acad Sci 860:318–332.

Smith JC, Feldman JL, Schmidt BJ. 1988. Neural mechanisms generating locomotion studied in mammalian brain stem-spinal cord in vitro. FASEB J 2:2283–2288.

Sqalli-Houssaini Y, Cazalets JR. 2000. Noradrenergic control of locomotor networks in the in vitro spinal cord of the neonatal rat. Brain Res 852:100–109.

Van Raamsdonk W, Bosch TJ, Smit-Onel MJ, Maslam S. 1996. Organisation of the zebrafish spinal cord: distribution of motoneuron dendrites and 5-HT containing cells. Eur J Morphol 34:65–77.

Vinay L, Brocard F, Pflieger JF, Simeoni-Alias J, Clarac F. 2000. Perinatal development of lumbar motoneurons and their inputs in the rat. Brain Res Bull 53:635–647.

Wullimann MF, Puelles L. 1999. Postembryonic neural proliferation in the zebrafish forebrain and its relationship to prosomeric domains. Anat Embryol (Berl) 199:329–348.

Wullimann MF, Rupp B, Reichert H. 1996. Neuroanatomy of the zebrafish brain: a topological atlas. Basel: Birkhauser.